Emilie Laache

Effectiveness of Debris Flow Breakers

Trondheim, June 2016

MASTER THESIS: TBA4900

Main supervisor: Professor Steinar Nordal

Co-supervisor: Harald Norem and Professor Vikas Thakur

Department of Civil and Transport Engineering

Norwegian University of Science and Technology (NTNU)

NTNU – Trondheim
Norwegian University of
Science and Technology

Preface

This Master thesis is written as a part of the MSc in Geotechnics and Geohazards at the Norwegian University of Science and Technology during the spring semester of 2016. The project is a cooperation between NTNU and the Norwegian Public Roads Administration. It is also a part of the Klima 2050 project and the Ferry Free E39 project. This thesis is a continuation of the specialization project "Effective Debris Flow Countermeasures" carried out in the autumn semester of 2015 by the author.

Trondheim, 2016-10-06

Emilie Laache

Acknowledgment

Summary and Conclusions

Debris flows are a hazardous geological phenomenon occurring in mountainous terrain. In Norway the National Public Road Administration has registered around 1060 debris flows since the 1970's. The damages caused by a debris flow can be severe and sometimes tragic. Countermeasures are therefore used to protect communities, infrastructure and agriculture from its large destructive powers. Debris flow breakers are a countermeasure developed in Japan, but is not commonly used as local residents tend to be distrustful of its design. It is designed as a drainage screen placed horizontally over the river bed where its purpose is to drain out the water from the debris flow that flows over. By removing the water the excess pore pressure along the shear surface is dissipated which then causes the debris flow to stop. This countermeasure is not mentioned in the NPRA's guidelines for debris flows and debris flow countermeasures, and there are only Japanese studies on the effectiveness and design of the debris flow breakers.

To investigate the effectiveness of the debris flow breakers 27 tests were carried out on a physical debris flow model. First, three reference tests with no countermeasures were done. Then, 6 tests with two solid plates were conducted to investigate the effect of placing the breakers horizontally out of the channel instead of integrating them into the channel. Finally, 18 tests were done with 6 different breakers with the lengths 0.5 and 1.0 m and 2, 4 and 6 mm opening widths. Their effectiveness was evaluated in terms of reduced runout compared to the reference tests.

The interaction between the debris flow and debris flow breaker appeared to be as the theory suggested. Water drained through and the debris flow front or body

stopped on top of the breaker, depending on the length of the breaker. As a result of the stopped debris flow masses the following part of the debris flow flowed into the stopped masses and stopped as well. This damming effect caused the debris flow masses to accumulate upstream while the water drained through the dry masses and breakers. This upstream deposition height increased as the opening width of the debris flow breakers decreased. This was due to the amount of material that could pass through the different opening widths, the smaller opening the less material could pass and therefore accumulated upstream.

The results showed that the most effective debris flow breaker was 1.0 m long and had 2 mm opening widths. This breaker had a 76% effectiveness. All the 1.0 m long breakers had an effectiveness between 73-76% and were more effective than the 0.5 m long breakers whose effectiveness was between 23-41%, the 2 mm opening widths being the most effective. The 1.0 m long breakers were also more effective than all the other countermeasures tested in the same model before. These countermeasures included a check dam, slits dams and baffles. In conclusion, the results from the physical modeling of the debris flow breakers indicate that they are an effective countermeasure that can be trusted and should be used.

Contents

List of Figures

List of Tables

Chapter 1

Introduction

Debris flows are a hazardous geological phenomenon occurring in regions with step mountainous terrain that experience occasional rainfall. The triggering of a debris flow is often related to extreme weather, especially heavy precipitation. Climate research indicate an increase of extreme weather events in the future, which suggests that debris flows are more likely to occur. Debris flows contain water and occur periodically in establishes paths, usually rivers, gullies or drainage paths. It is considered to be one of the most hazardous landslide types due to their poor predictability, high flow velocity, high impact forces and long runouts. The damages they may cause can be severe and sometimes tragic. Infrastructure, communities, agriculture and human lives are all vulnerable to the destructive powers of a debris flow. In order to protect them, countermeasures or mitigation measures are placed such that they can stop the debris flow or reduce the damages. Non-structural countermeasures also called soft countermeasures are equally important as structural countermeasures and include regulation of hazard-prone areas and the avoidance of risk by taking refuge. In Norway there has not been a systematic approach to implement structural

debris flow countermeasures. Also, little is documented about the effectiveness of the different countermeasures available, which makes it difficult to assess which to use. This has resulted in engineers choosing countermeasures based on experience instead of documented design criteria and calculations. Since the 1970's, 1060 debris flows have been registered by the National Public Road Administration (NPRA), many of which have caused damage Lygre (2014). Therefore, as long as debris flow events occur, but cannot be predicted, documented effective countermeasures are essential to provide security.

1.1 Background

One of the oldest torrent control structures recoded was built by the prince-bishop Bernardus Clesius in 1537 in Italy (Armanini et al., 1991). Over the years different countermeasures have been built, some more effective than others. Possibly the most known and used debris flow countermeasure is the check dam, which is a vertical solid dam structure. Other used countermeasures are deflection structures, flexible barriers, channels and baffles. Also more innovative countermeasures have been designed, as the debris flow breaker. This countermeasure has only been studied in Japan so far and is not mentioned in the Norwegian guidelines given by the NPRA for debris flows and debris flow countermeasures. The few conducted studies indicate that they are an effective countermeasure. However, local residents in Japan tend to be distrustful of its effectiveness due to its design. More research and information on the breakers could possibly change this view, and also make the breakers a countermeasure used in Norway and other countries.

1.2   Objectives

The objectives of this work is to

1. understand the physics of debris flows using a physical model

2. test debris flow breakers as a countermeasure in a physical model

3. study the interaction between debris flows and debris flow breakers

4. study the optimal length, opening width and percentage opening of the debris flow breakers

5. evaluate the effectiveness of debris flow breakers as a countermeasure

6. compare debris flow breakers to other countermeasures tested in the same physical model

1.3   Structure of the Report

The rest of the report is structured as follows: Chapter 2 gives an introduction to debris flows and debris flow countermeasures while chapter 3 describes debris flow breaker more in detail. Chapter 4 describes the experimental set up, the model, material and debris flow breakers used for the experiments. Chapter 5 presents the results and analysis from the experiments while chapter 6 discusses the results in light of the objectives of this work. Chapter 7 is the conclusion and recommendation of

further work.

Chapter 2

Basics of Debris Flow and Countermeasures

Although debris flows have always existed, research on the behavior of debris flows started not that long ago. Around the 1960's researchers in Japan began to study the mechanisms and behavior of debris flows to understand how to protect themselves from its destructive powers. Other regions and countries around the world have also studied debris flows over the recent years, and Norway published their first guideline on debris flows and countermeasures in 2014. This chapter is a short summary on the basics of debris flows and different countermeasures in use today. A more detailed description is given in my specialization project "Effective Debris Flow Countermeasures".

2.1 Debris flow

Debris flows are a hazardous geological phenomenon that occur in regions with steep mountainous terrain that has at least occasional rainfall. The poor predictability

combined with characteristics as high flow velocity, impact forces and long runout, makes debris flows one of the most hazardous landslide types. Their great destructive powers may cause loss of human lives, damage to houses, agriculture and infrastructure which all may have great direct or indirect costs. Earlier, societies dealt with debris flow hazards through experience and by avoiding the most exposed areas. This is no longer a satisfactory approach as development proceed at a fast rate and does not allow sufficient time to build experience and understanding. As a result, in the late 1960s scientists started to research debris flows to understand its behaviour and characteristics, and since the 1970s the Norwegian Public Road Administration has registered around 1060 debris flows in Norway (Lygre, 2014).

In a debris flow there is both solid and fluid forces that act in concert which gives it unique destructive power. This is what distinguishes debris flows from rock avalanches and sediment-laden water floods where either the soil or fluid forces act. Debris flows often occur with little warning when masses of poorly sorted sediment saturated with water, surge down slopes in response to gravitational attraction. They may occur both on continental and seafloor environments where they can exert great impulse loads on objects they encounter. Hungr et al. (2001) defined "debris" as a loose unsorted material of low plasticity such as that produced by mass wasting process, weathering, glacier transport, explosive volcanism or human activity. Texturally, debris is a mixture of sand, gravel, cobbles and boulders, often with varying proportions of silt and a trace of clay. Debris may also contain a significant proportion of organic material, including logs, tree stumps and organic mulch. It is usually non-plastic or weakly plastic and its is characteristically unsorted, sometimes gap-graded (Hungr, 2005).

There are many ways to define debris flows, Takahashi (2014) defined it as: "a flow of sediment and water mixture in a manner as if it was a flow of continuous fluid driven by gravity, and it attains large mobility from the enlarged void space saturated with water or slurry", and Stiny (1910) said this about a observed debris flow "a viscous mass consisting of water, soil, sand, gravel, rocks and wood mixed together, which flows like a lava into the valley" (Hungr, 2005). There are different kinds of debris flows and different classification systems. Takahashi (2014) classified between two kinds of debris flows; the quasi-static and the dynamic debris flow. The quasi-static debris flow is where the Coulomb friction stress dominates and may only occur when its solid concentration is more than the threshold value of about 0.5, while the dynamic debris flows occur at a lower solid concentration than the quasi-static. If the concentration is higher than 0.5 neither dynamic nor quasi-static debris flow may occur. This is due to the absent particle dislocation within the body which makes it rigid. Bagnold (1954) gives this threshold value to be 0.56 for beach sand. It is the dynamic debris flow that is the used and most relevant kind of debris flow, and there are three different kinds of dynamic debris flows:

- **Turbulent-muddy type debris flow** is where the turbulent mixing stress dominates. This type of debris flow is mainly comprised of fine ash, although they may contain many large boulders. It acts almost as a flow of water as it is wet and the particles are set to move due to turbulence in the water. These kinds of debris flows often occur in volcanic areas and near glaciers where fine grained material can be found. In order for a debris flow to have such turbulence to carry out materials and have enough transport capacity it has to have a limited amount of material mass relative to the water masses. Therefore, turbulent de-

bris flows are unlikely to have greater volumetric density than 30%, and 75% of the particles have a diameter less than 1 mm Takahashi (2014).

- **Viscous debris flow** is where viscous stress dominates. This debris flow has a higher volumetric density than the turbulent. This is due to smaller space between the particles and hence less movements. According to Takahashi (2014) the mass density is normally 1.8-2.3 t/m^3. To achieve this density it is essential that the debris flow erodes mass as it develops.

- **Stony-type debris flow** is where grain collision stress dominates. This debris flow behaves like the viscous debris flow, only with bigger sediments in front and on the sides as a wave front. The large material will be around 50-70% of the debris volume while the fine material is about 10-20%.

In Norway the NPRA classifies between two types of debris flows, turbulent and fully developed debris flows (Statens Vegvesen, 2014). The fully developed debris flow is characterized by a higher volumetric density than the turbulent debris flow. This means that there is less movement and smaller space for the particles to move which makes the flow act like a continuum of water and particles. In relation to the Takahashi classification, the fully developed debris flow covers both the stony type and the viscous type. These two classifications are only two of many, but they are the ones that will be considered in this master thesis.

The flow path of a debris flow is usually divided in three different parts; the source

area, transport area/channel and the deposition area, this is illustrated in figure 2.1. The source area is where the debris flow starts and the main process is erosion or an initial landslide. Usually the debris flow velocity will accelerate in this area. In the transport channels the debris flow usually reach its terminal velocity and there is transport of material but often also entrainment of new material so that the debris flow volume increases. However, in steep turns or in flattening terrain sedimentation may occur. In the depositional area the debris flow decelerates and sedimentation occur. The coarse material is usually deposited first and then the finest material may even deposit beyond the deposition area.
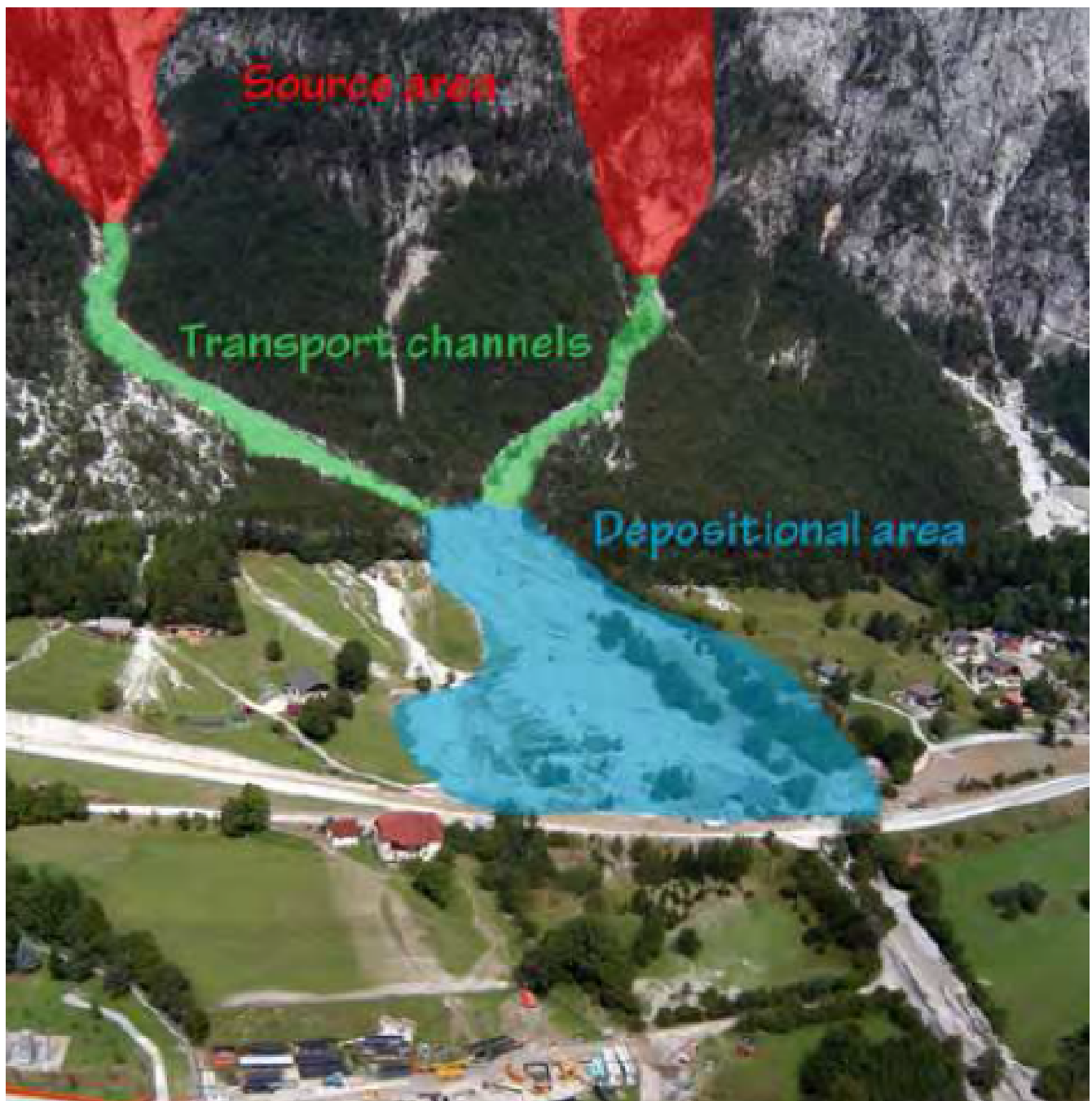
Figure 2.1: The main part of a debris flow path (Calligaris and Zini, 2012)

It is known that debris flows derive most of their volume by entraining loose saturated material from their path (Hungr et al., 2005). Thomas and Goudie (2009) defines entrainment as:

"the process by which surface sediment is incorporated into a fluid flow (such as air or water) as a part of the operation erosion. Sediment is entrained into a flow when forces acting to move a stationary particle overcome the forces resisting movement"

If a debris flow entrain sediment by scouring channel beds or undermining channel banks it can become especially mobile and destructive (Hungr et al., 2005). This is caused by an increased volume, speed and runout. Iverson et al. (2011) conducted a physical experiment to investigate the entrainment process. Here they released a 6 m^3 water saturated debris flow across a 47 m long and 12 cm thick bed of partially saturated sediment. For each debris flow they measured the evolution of flow thickness, basal total normal stress, basal pore-fluid pressure, and sediment scour depth. What they found was that entrainment occurred by rapid (5-10 cm/s), progressive scour rather than by mass failure at depth. Overriding debris flows rapidly generated high basal pore-fluid pressures when they loaded and deformed bed sediment, and in wetter beds these pressures approached lithostatic levels. Reduction of inter granular friction within the bed sediment thereby enhanced scour efficiency, entrainment, and runout. However, if dryer bed sediment was entrained, the feedback became negative and flow momentum declined.

According to Statens Vegvesen (2014) there are mainly two triggering mechanisms of debris flows. One of them is when the shear stress from a water flow exceeds the shear strength of the underlying layer, resulting in failure and sediment transportation. If the erosion velocity and transportation capabilities of the water is high enough then the content of sediment in the water will gradually increase and de-

velop into a debris flow. Most of the documented cases of debris flows in Norway are triggered by this (Statens Vegvesen, 2014). The other triggering mechanism is when a landslide or snow avalanche slide out and manages to release water so that the mixture of water and sediment reaches a sufficient mobility. Figure 2.2 is an illustration of the two triggering factors, and two specific examples of each.
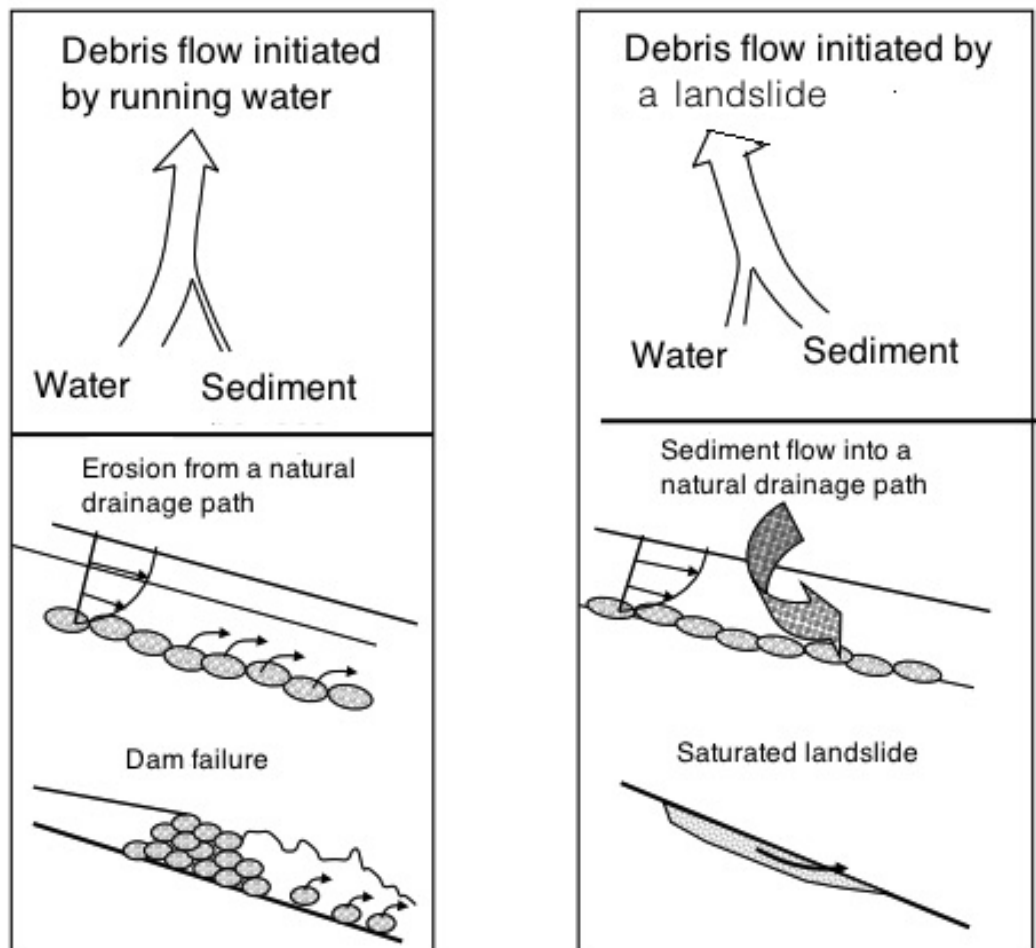
Figure 2.2: The different triggering factors and their mechanisms (Statens Vegvesen, 2014)

In comparison to how the Norwegian Public Road Administration defines the triggering factors, Takahashi (2014) says that debris flow initiation can be classified into three types:

- Erosion of gully bed by the supply of water from outside until the concentration

of solids in the surface water flow become as dense so that is can be called a debris flow

- A landslide transforms into debris flow while in motion by the effects of storage water in the landslide or by the supply of water outside

- A sudden collapse of a debris dam

The difference between Takahashi's and NPRA's classifications is that NPRA considers the collapse of a debris dam as the same as shear stress from water exceeding the shear strength of the underlying layer.

A method to graphically present the debris flow velocity and energy in a debris flow is through energy lines. An energy line is a line that represents the total head available to a fluid. It can be used as a graphical tool/model to describe the movement of any avalanche or landslide. It is common in evaluating the energy dissipation along the streamline. The Bernoulli equation says that the energy remains constant along a stream line for a steady inviscid, incompressible flow and is expressed as:

$$\frac{v^2}{2} + gz + \frac{p}{\rho} = constant \tag{2.1}$$

where

v = velocity

g = acceleration due to gravity

z = elevation

p = pressure

ρ = density

For debris flow the equation can be simplified in terms of total head or energy head H.

$$H = z + h + \frac{v^2}{2g} \tag{2.2}$$

where

z = elevation [m]

v = velocity [m/s]

g = acceleration due to gravity (9,81 $[m/s^2]$)

h = flow height [m]

The energy line is then a line that represents the energy head available to the fluid along the flow path. The potential energy is then equal to the elevation and the kinetic energy is equal to $\frac{v^2}{2g}$ which is also called the velocity head as seen in Figure 2.3.
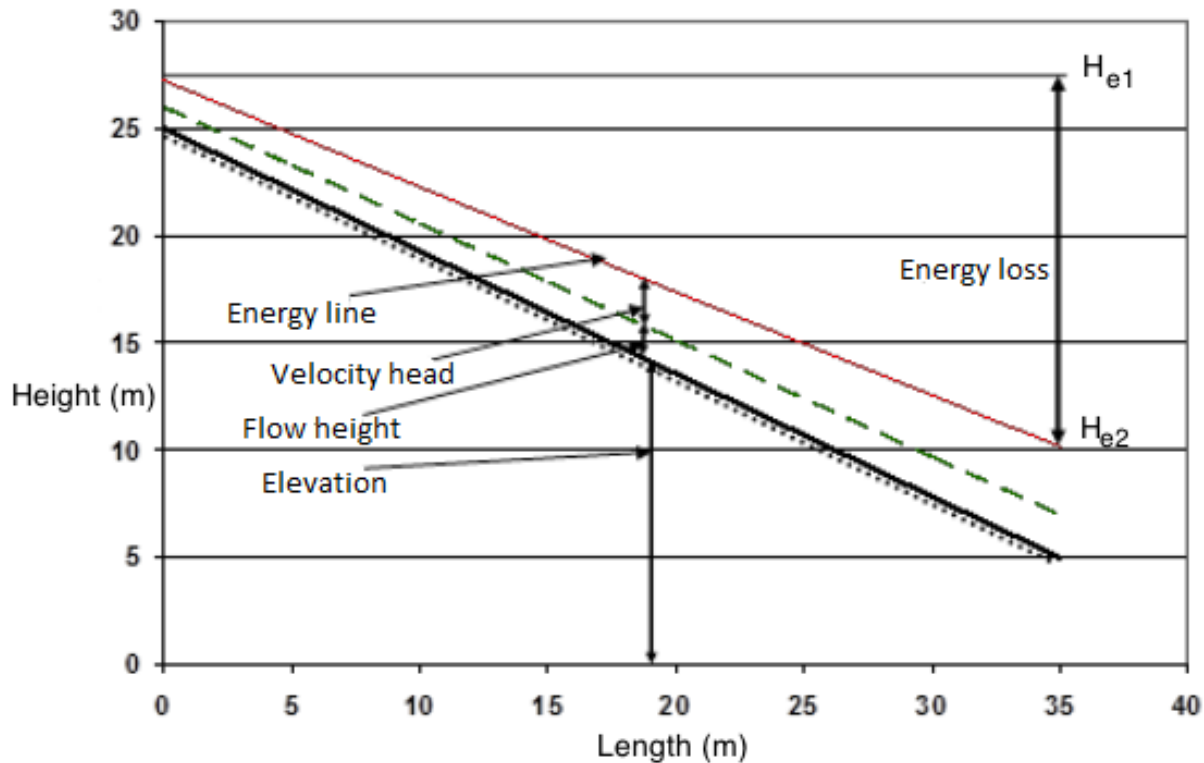
Figure 2.3: An energy line example showing the different parameters in the energy line/total head (Statens Vegvesen, 2014)

This is one of the methods presented in the guidelines for debris flows given by the NPRA.

2.2 Pore Pressure

As seen, water plays a major role in initiation and behaviour of debris flows. The initiation can often be seen in relation to meteorological conditions, in particular extreme weather events such as major storms with heavy rainfall, either short intense precipitations, or rain accumulation over a longer period of up to 15 days (Sandersen et al., 1997). The short intense precipitation cause surface erosion while the rain

accumulation over a longer time gives a slow build up of pore pressure, both being triggers to debris flow. The pore pressure build up is very essential in the behaviour and triggering of debris flows. Earlier it was assumed that it was mostly loose sediments that could develop into debris flow because these sediments experience a reduction in volume during shear stresses and due to volume change the sediment has to dispose any excess pore water. However, later experiments (Sassa et al., 2007) have shown that dense sediments may also develop into debris flow as rapid deformation causes less contact between grains causing high pore pressures that can carry the weight of the landslide. An other cause of rapid accumulation of pore pressure short time after the initiating landslide may be the rapid loading of the ground under the landslide. Sassa et al. (2007) explained the rapid pore pressure and erosion as a loading happening as an undrained loading. When a landslide slides over drained soil both the weight and the increased pore pressure will cause reduced stability for the whole sediment and result in severe erosion. This is shown in figure 2.4 below.

It is believed that pore fluid pressures larger than hydrostatic values are an important factor that contributes to the commonly long runout distances of debris flows. This excess pore pressure reduces the strength of the flowing material which causes the long runout distances. The high pore pressures along the shear surfaces reduces the energy loss which contributes to the long runout. There are several experiments and studies that support this hypothesis.

Major and Iverson (1999) generated experimental debris flows of about 10 m^3 volume at the U.S. Geological Survey (USGS) debris-flow flume to investigate the pore pressure in debris flows. What they found was that the debris flow front surge exhibited negligible positive pore fluid pressure while the debris masses behind the front
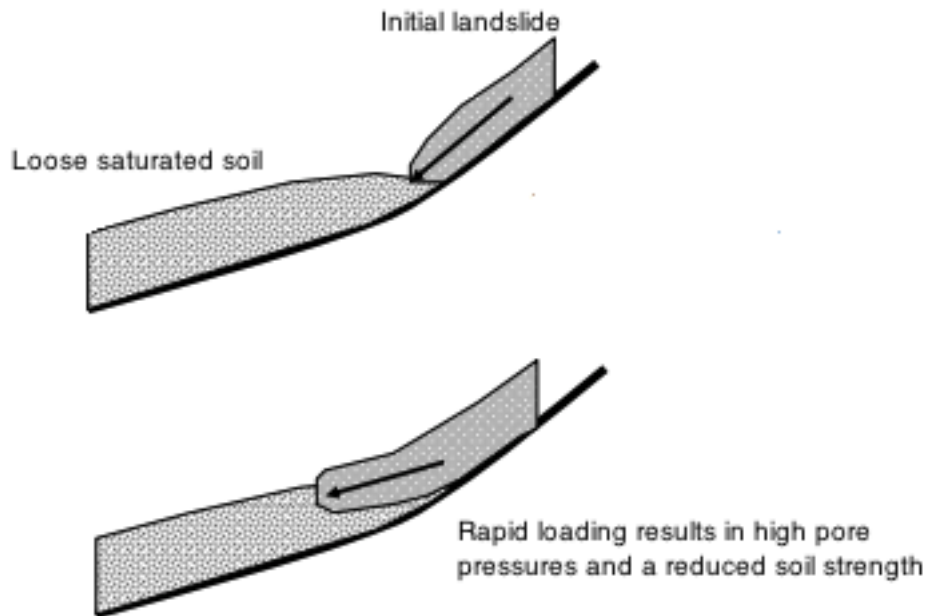
Figure 2.4: An illustration of the process that may cause an initial landslide to develop into a debris flow when flowing over loose saturated soil. This soil experience rapid loading which result in high pore pressured and reduced soil strength. (Statens Vegvesen, 2014).

had pore-fluid pressures nearly sufficient to cause liquefaction. This was observed during mobilization and acceleration of the flow and persisted in the debris flow interior during deceleration and deposition. This excess pore pressure only dissipated significantly during post depositional sediment consolidation. In conclusion they said that debris-flow deposition results from grain-contact friction and bed friction concentrated along the flow perimeter, where high pore-fluid pressure is absent.This study by Major and Iverson (1999) supports Iverson (1997) earlier observations of measured basal fluid pressures, which indicate that the debris flow front surges generally lack much fluid pressure, whereas the finer-grained tails of surges are nearly liquefied by high fluid pressure. Interior fluid pressures remain elevated at nearly liquefaction levels even during deposition, indicating that deposition results mainly from resistance at flow heads and margin. McArdell et al. (2007) found the same results that support the idea that excess pore fluid pressures are long lived in debris

flows. They observed that excess pore fluid pressure were present over most of the duration of the flow and this contributes to the unusual mobility of debris flows.

Wang and Sassa (2003) did some physical experiments to investigate the pore pressure generation effects of grain size and fine particle content. Among their results they found that pore pressure within saturated sand increased with the moving velocity and finer grains started to float at slower moving velocity.

2.3 Debris Flow Countermeasures

Countermeasures for debris flow may be divided into two categories, structural- and non-structural countermeasures. The structural countermeasures are countermeasures that need some engineering work, but also tree planting may be categorized as a structural countermeasure. The structural countermeasures are often considered the most important ones. However, the non-structural or soft countermeasures such as regulation of developing hazard-prone areas and the avoidance of risk by taking refugee is equally important. Below is a summarized short version of the mentioned countermeasures in Laache (2015), but debris flow breakers will be presented in more detail in chapter 3.

Check Dams

Check dams are constructed to decrease sediment peak discharge and the total volume of sediment outflow to the downstream area. This type of countermeasures is often used in rivers or channels where debris flow and sediment transportation often

occur. They can be used in singles or in series. The most used kinds of check dams are the open and closed type. Both are traditional structures meant to control debris flow either permanent or temporary. Figure 2.5 shows three different types of check dams, slit dam, grid dam and closed check dam. The slit- and grid dam are open check dams.

Figure 2.5: The left picture is a concrete slit dam in Madeira, Portugal (LCWConsult, 2015). The middle picture is a grid dam (nip) and the right picture is a series of closed check dams (Remaître et al., 2008).

Closed check dams reduce the sediment transportation to the downstream river reaches and stabilize river beds. They can be permanent or temporary with the intention of slowing down the velocity of water and prevent erosion and promote sedimentation. Japan has more than 85,000 debris flow prone torrents and approximately 20% of these torrents who has more than five houses or public buildings downstream contain at least one check dam (Takahashi, 2014).

Open check dams are commonly used for two purposes, to reduce the kinetic energy of the flow or temporarily store debris flow volume. When trying to reduce the kinetic energy of the flow, the open check dams are usually located in the upper part of the flow path where the available volume is small. For the other case where the purpose is to temporarily store debris volume the check dams are located at the lower part of the flow path. The open check dams allow a continually supply of safe and neces-

sary sediment downstream through large openings in the dam body which prevents a buildup of bars behind the dam which is often a problem when using closed check dams. Through the openings sediment runoff from normal flood flows are allowed to pass while it works as a closed not yet filled check dam when a debris flow occur.

Debris Flow Baffles

Baffles are usually used in arrays and may be installed in front of a rigid barrier where the aim is to reduce the flow velocity just before impact. They can also be installed in an open stream course where the aim is to control the flow discharge. Both cases can be seen in figure 2.6. The functionality of baffles arrays is to perturb the flow pattern such that the flow slows down as it approaches each block, and then accelerates towards the next row to accommodate the dissipation of flow energy upon impact (Choi et al., 2014).
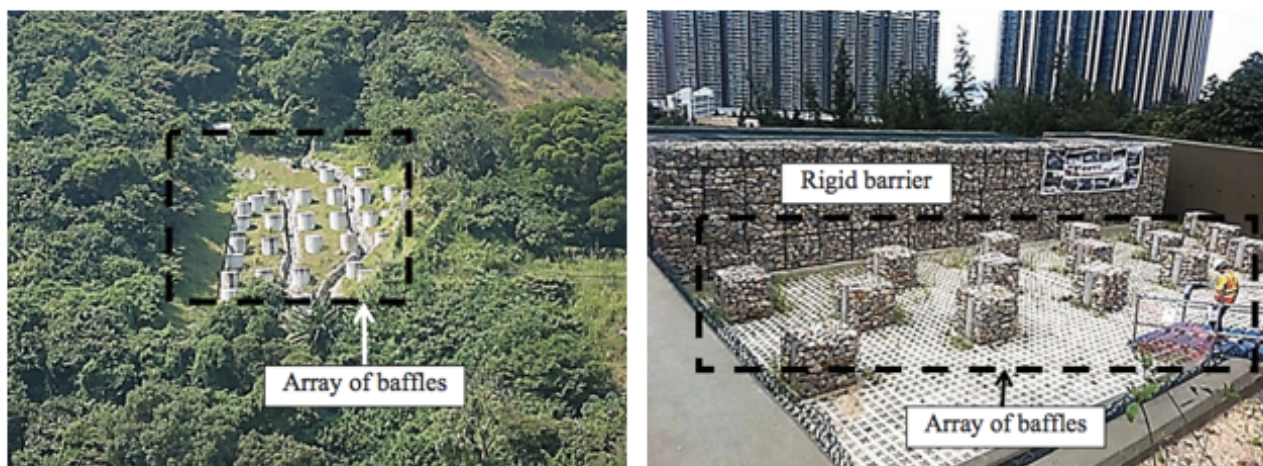
Figure 2.6: The left picture shows debris flow baffles in arrays in an open channel in Kennedy Town, Hong Kong. The right picture shows arrays of baffles in front of a rigid barrier in Lantau Island, Hong Kong. (Choi et al., 2014).

In the case where baffles are used to control the discharge it is imperial to prevent overflow to ensure that the debris is gradually discharged through the baffles downstream instead of passing uncontrolled over the baffles arrays.

Deflection Structures and Channels

A deflection structure can be a dike, wall or groyne, all with the same intention of directing the debris flow to an area of low economic cost. They are usually the last element in a systematic prevention system where they are to control any remaining risk. However, they can also be used in the transport area, but the requirements for impact and erosion control is higher in this part of the flow path.
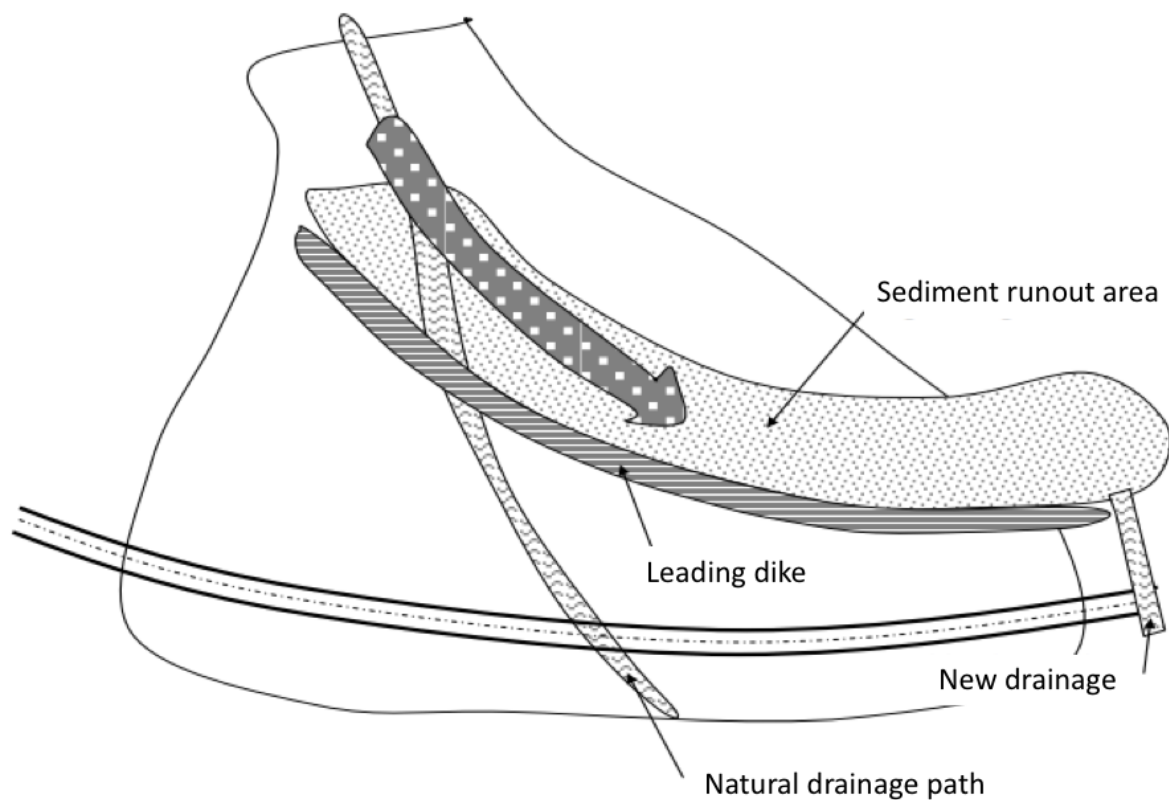
Figure 2.7: Illustration of a deflection structure that protects the road by leading the debris flow to a planned area for it to deposit safely and without damaging the road. (Statens Vegvesen, 2014)

Figure 2.7 illustrates a deflection structure leading the debris flow away from the road and to a planned deposition area where it will not cause any harm. The old drainage path, the natural, is closed off and a new one is created in the sediment runout area.

Channels are used to channelize the debris flow to prevent it from spreading out or flow over unwanted areas. Figure 2.8 illustrates this principle where the channel is preventing debris flow from damaging the surrounding houses.
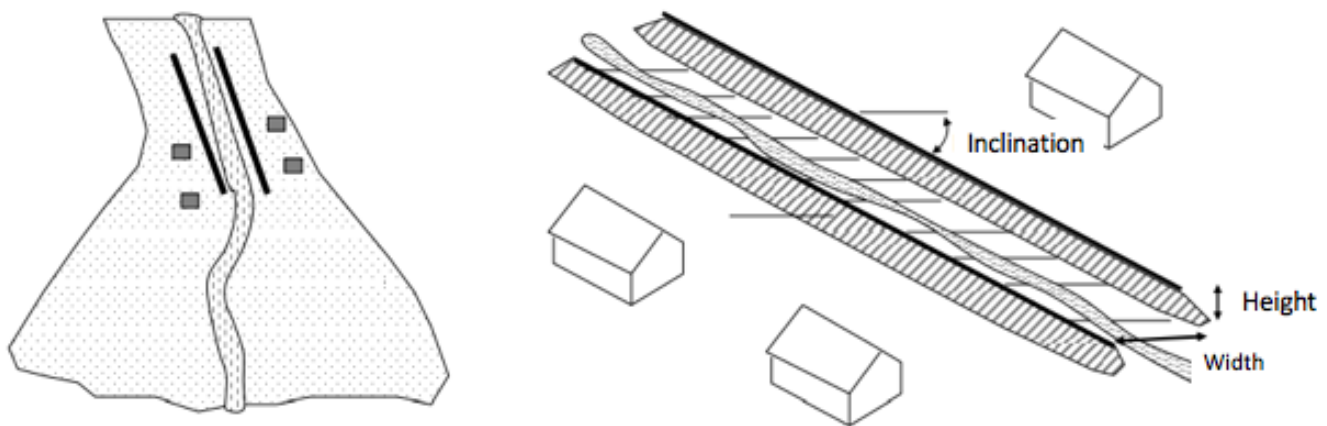
Figure 2.8: Illustration of the usage of channels to safely guide the flow past vulnerable areas (Statens Vegvesen, 2014)

When using channels the slope has to be steep enough so that the flow continues to move without any significant velocity reduction. This is to avoid any over topping of the channel walls. The channels should therefor have a steady slope and be as straight as possible. VanDine (1996) observed little sedimentation in channels where the slope was steeper than 12°, but the slope should preferably be steeper than this.

Flexible Barriers

A flexible debris flow barrier is a steel net supported by lateral ropes which are anchored to the ground. Figure 2.9 shows a multi-level flexible barrier system that has successfully stopped a debris flow in the Merdenson torrent in Switzerland. A free passage is often constructed between the lower net and the river bed where the normal flow may pass without causing any damage. This free space also provides a passage for animals where large nets are constructed. The height of the net typically range from 2 to 6 meters depending on the size of the torrent (Volkwein, 2014).

Figure 2.9: A multi-level flexible barriers in the Merdenson torrent in Switzerland after stopping a debris flow (Volkwein et al., 2011).

In Norway this form of prevention is commonly used for rock fall, not debris flow. Rock fall and debris flow have the same main dynamic force, however the forces in debris flows is distributed and acts in surges. In addition to the distributed loads

there are also single impact loads from individual boulder. Both these loads are transmitted to margins and support structures that must also resist. To avoid failure it is important to consider aspects like ropes, anchoring, support, abrasion, retention volume and energy absorption (Volkwein et al., 2011). If failure where to happen it could lead to catastrophic consequences because of the large trapped volume. This volume would then be released causing an increase in the disruptive potential.

Chapter 3

Debris Flow Breakers

Debris flow breakers are a countermeasure developed in Japan which consists of a screen placed horizontally over the riverbed as seen in figure 3.1. The countermeasure is not mentioned in the Norwegian guidelines for debris flows and debris flow countermeasures, and there is limited research on the field elsewhere in the world. However, the research that do exist indicate that the breakers are an effective mitigation measure for debris flows. It is therefore of great interest to study this countermeasure to see if it is suitable in the Norwegian context. In Japan, debris flow breakers are considered cost-efficient, simply designed and easily repaired and maintained. Despite all that, debris flow breakers are not a commonly used countermeasure as local residents tend to be distrustful of their efficiency. They prefer preventive measures that look more solid, like check dams (Mizuyama, 2008). More research and information on the breakers could possibly change this view, and also make the breakers a countermeasure used in Norway and other countries.

Debris flow breakers are constructed upon the principle that a debris flow will stop

moving if water is removed from the flow. It is not the water itself that makes the debris flow move fast and for long distances, but rather the excess pore fluid pressure as discussed in chapter 2. By removing the water this excess pressure will dissipate. As mentioned in chapter 2, excess pore pressure contributes to the high velocities and destructive powers of a debris flow. The excess pore pressure creates low effective stresses which allows the debris flow to flow with high velocities without losing much energy along the shear surface. By removing the water from the debris flow the excess pore pressure will dissipate and cause energy loss which will make the debris flow stop. Figure 3.1 illustrates this principle of the debris flow breaker. The debris flow has high pore fluid pressures before flowing over the breaker, but as the debris flow flows over the breaker water drains through the breaker and the pore fluid pressure decreases. This causes the debris flow to stop..
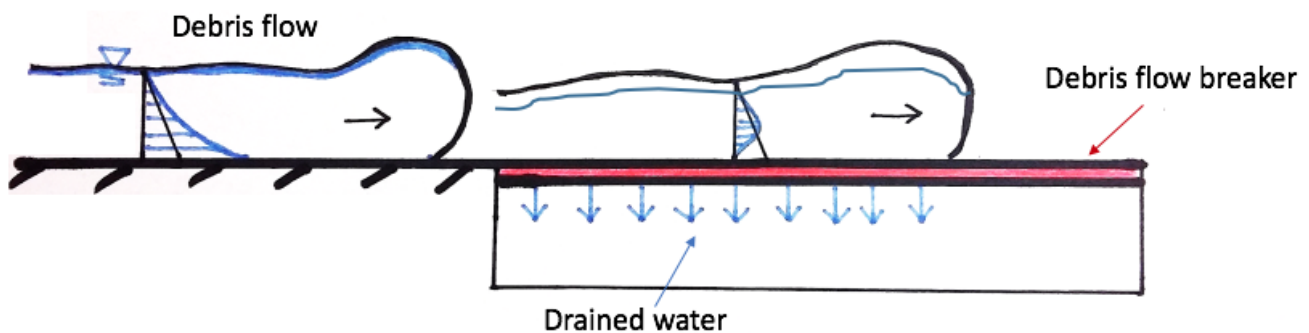
Figure 3.1: Illustration of the principle of the debris flow breaker. The pore fluid pressure (the blue line) is higher than hydrostatic (the black line) before it flows over the breaker, and lower than hydrstatic on top of the breaker as the pore water drains out of the debris flow throught the breaker. This causes the debris flow to stop.

The debris flow breaker have existed since 1956 when Professor Noriaki Hashimoto of the Nagoya Institute of Technology conceived the idea of debris flow breakers. It was tested and verified by the Public Works Research Institute in three pilot projects in Japan. This was done to gather information about construction and maintenance.

Later on, a full scale project was carried out at mountain Tokachidake in Kokkaiodo, Japan (ICHARM, 2008). Debris flow breakers have also successfully been used during two volcanic torrents in Japan (Mizuyama, 2008). Figure 3.2 shows a debris flow breaker in the Kamikami-Horisawa Valley, Mount Yakedake before and after a debris flow. Similar to most debris flow countermeasures, the debris flow breakers also require maintenance and clean up after a debris flow event in order for it to act sufficient for any following debris flows.

Figure 3.2: A 20 meter long and 10 meter wide debris flow breaker in Mount Yakedake, Japan. The left picture is before a debris flow has occured while the picture on the right is after stopping the debris flow (Mizuyama, 2008)

Illustration of the debris flow breaker screen and its parameters which are the length, width, opening width and blocking width is given in figure 3.3. The opening width also determines the percentage opening of the breakers which is

$$\text{Percentage opening} = \frac{\sum w_o}{W} \tag{3.1}$$

where

w_o = the opening width $[m]$

W = Total width of the debris flow breaker screen [m]

For the breakers that has been built out in the field like in figure 3.2 the blocking width and the opening width has been 20 cm. This gives a 50% opening. The screen of these breakers are constructed of square beams. It is important that the screen can withhold the weight of the flowing debris flow because a collapse of the screen would destroy the effect of the countermeasure.
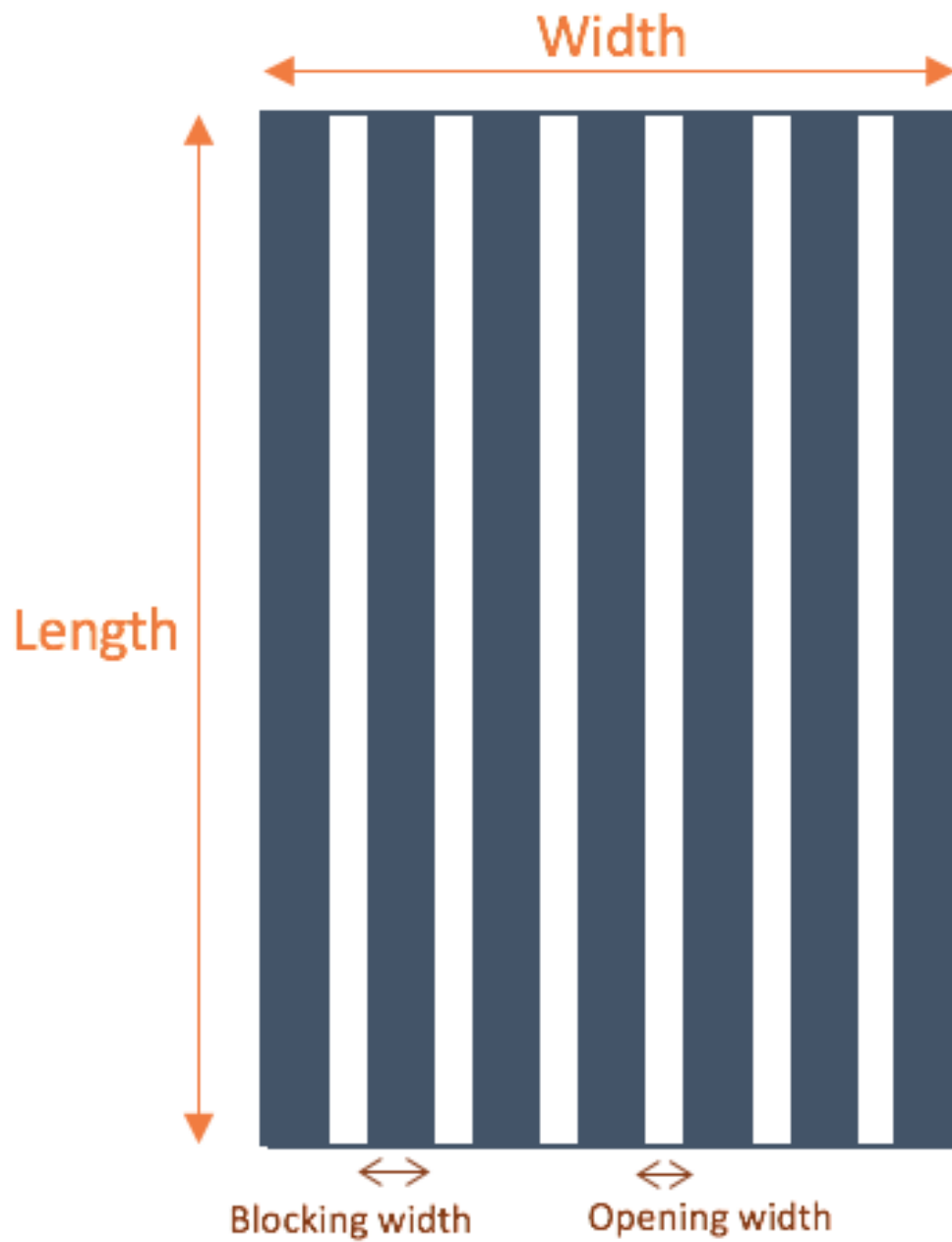
Figure 3.3: The different parameters that may vary on a debris flow breaker is the length, width, opening- and blocking width. These parameters also influence the percentage opening of the debris flow which is the total opening divided by the total area of the screen.

3.1 Physical Experiments and Modeling of Debris Flow Breakers

There are only two articles on debris flow breakers in English. These are studies involving physical and numerical modeling of debris flow breakers, both from Japan. Gonda (2009) developed a numerical model for debris flow breakers and conducted physical experiments to test the numerical model. Six types of breakers with different strip openings were tested using three different materials. However, the material used was nearly uniform gravel which is not representative for a real debris flow event. The debris flow volume used was 7000 cm^2 and the openings were 0, 1, 2, 4, 8 and 12 mm while the slope was 16° and 19.7°. The channel length was 335 cm and had a width of 20 cm, the model can be seen in figure 3.4.
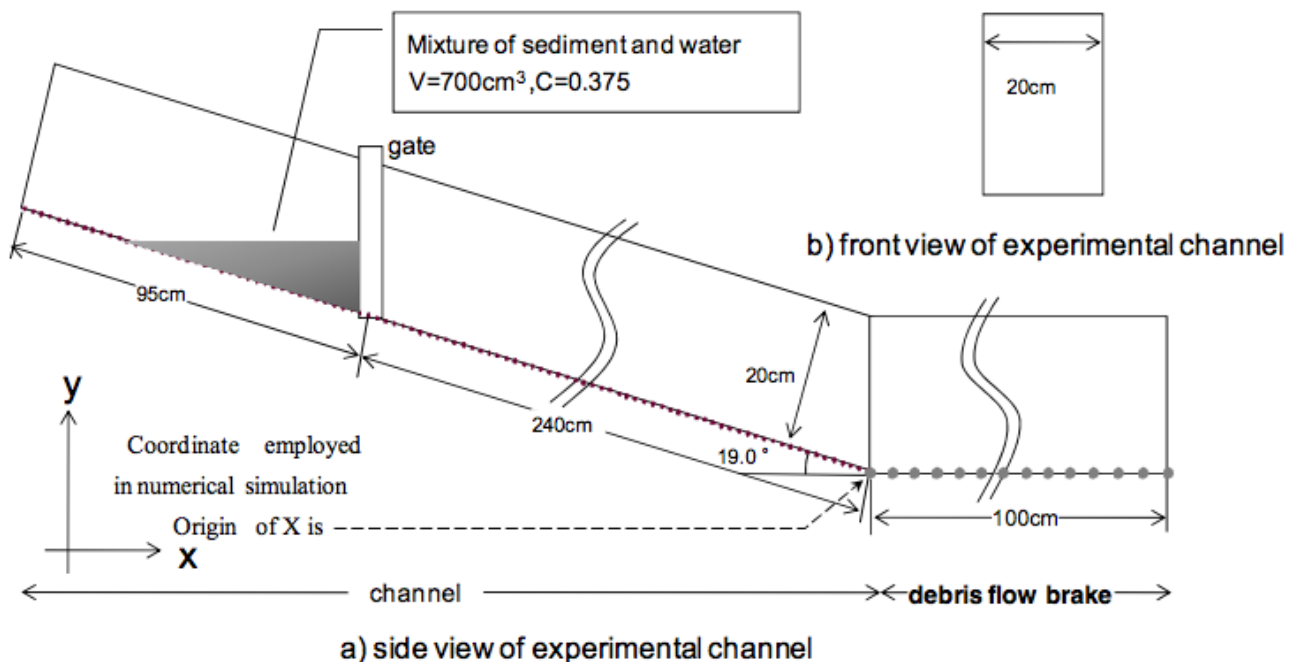
Figure 3.4: Illustration of the physical model of the debris flow channel (Gonda, 2009)

In this experiment they measured the travel length of the debris flow over the debris flow breaker. What they found was that the travel length decreased as the size of the openings increased. However, when the openings exceeded a certain width the travel

length remained constant. This threshold value, S*, increased as the diameter of the material increased. This is seen in table 3.1.

	d [mm]	S_* [mm]
Material A	1.8	1.1
Material B	3.4	1.3
Material C (16°)	4.7	2.4
Material C (19.7°)	4.7	2.4

Table 3.1: The treshold value for the debris flow breakers openings of the different materials.

For material C they also tested two different slopes (16° and 19.7°). They found that the threshold value S* was almost equal for the two different slopes, indicating that the slope did not play a major role in the S* value.

The drawn conclusion from the numerical and physical modeling was that the change in pore water pressure dominated the behaviour of the debris flow, not the change in concentration due to drainage of pore water through the debris flow breakers. This conclusion supports the theory presented in chapter 2 on the excess pore fluid pressures being the causes of the high velocities and long runouts.

Kim et al. (2012) continued the work of Gonda (2009) and conducted similar experiments only they did not use uniform gravel. They also changed one of the factors in the numerical model developed. Kim et al. (2012) tested three different materials to find the most effective combination of blocking size and opening size. They found the 10 mm blocking and 6 mm opening to be the most effective. The combination which gave the poorest result was 60 mm blocking and 2 mm opening. These results suggest that the percentage opening has a high impact on the effectiveness of the debris flow breakers. From their analysis they found that to achieve a 50% reduction in the travel length the percentage opening had to be bigger than 19-24% (depending on the sediment). They also found that the opening had to be 1.1-1.3 (depending

on the sediment) times the d_{95} (the 95 percentile diameter size of the material) to achieve a 50% reduction of the travel length.

The numerical model developed by Gonda (2009) and Kim et al. (2012) both have the assumption of hydrostatic pore pressure in the debris flow before the debris flow flows over the breaker. Figure 3.5 illustrates this assumption in the numerical model.
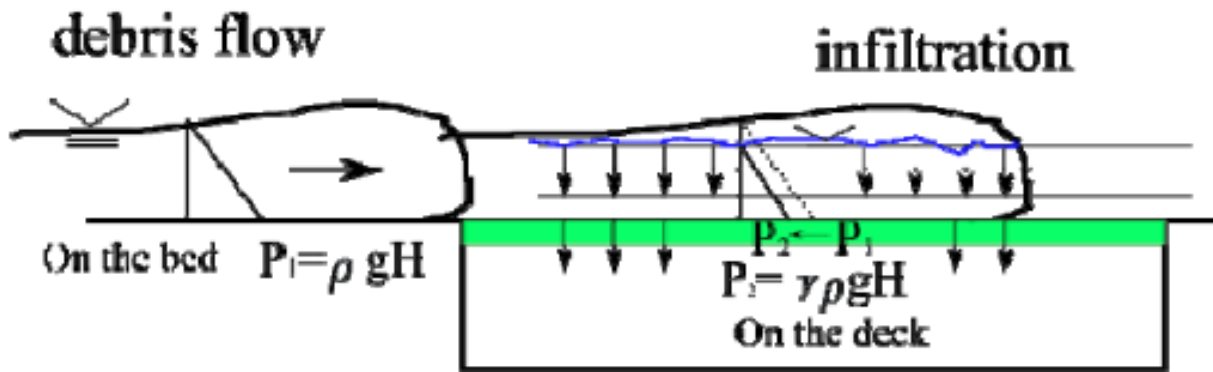
Figure 3.5: Illustration of the hydrostatic pore pressure in a debris flow before it flows over the breaker. An assumption made for the numerical model by both Gonda (2009) and Kim et al. (2012). (Kim et al., 2012)

This assumption of hydrostatic pore pressure in a debris flow does not agree with the theory presented in chapter 2. Research done on the pore pressure in debris flows suggest that it is only in the debris flow front that the pore pressure may be hydrostatic. In the internal body the pore-fluid pressure is often nearly sufficient to cause liquefaction. Due to this assumption and limited time it was decided not to look any closer at the numerical model, but focus on the physical modeling instead.

3.2   Similar Structures

It is not unknown to use screens or grids to block out unwanted material from a flow. Jernbaneverket, the Norwegian government's agency for railway services, are using something they call self-cleaning grids. These have some similarities to debris flow breakers, but are not intended to be used for debris flow but water flows. The grids are used in front of culverts where clogging during flooding may occur. The clogging is often caused by earth, threes and stones transported by a stream during flooding. Intensive rainfall can even cause small streams to transport masses. These masses then end up clogging the culvert partly or completely which in short time can result in over-flooding. The over-flooding may cause great damages to roads or railways. Figure 3.6 shows these self cleaning grids in Langhelle for low and high flows. These self cleaning grids have been installed several places in Voss municipality where they are very pleased with their effectiveness. However, neither hydraulic or hydrological assessments have been done.

Figure 3.6: Self cleaning grids in Langhelle. On the right is the self cleaning grid during a flooding (Photo: John Endre Fossmark) and the left when there is normal flow (Photo: Jeanette Gundersen).

These self cleaning grids are used in other places in the world, but called bottom rack intake. Kim (2013) did a literature review where he looked at the hydraulic behaviour and description of these grids for his study on debris flow breakers. The general conclusion he found by looking at studies conducted by Brunella et al. (2003), Orth et al. (1954), Ract-Madoux et al. (1955) and Kuntzmann and Bouvard (1954) was:

- knowledge of the water and sediment discharge is important for the design

- the rack should be constructed with rounded profiles in the stream direction

- The bottom slope of the rack should be more than 20% to obtain minimum risk of sediment clogging

- Acceptable rack spacing for mountainous regions is 0.10 m

These studies are restricted to rectangular channels with an opening in the bottom made of racks. The purpose of the bottom racks is to divert sediment and to produce an intake structure in which sediment sizes larger than the bar spacing are excluded. Neither of these studies involve debris flows, only water, and a debris flow is more complex than a pure water flow.

Chapter 4

Physical Model and Experimental Setup

To test the effectiveness of the debris flow breaker 27 physical experiments were planned. Different lengths, opening widths and percentage openings were to be tested to find the most effective debris flow breaker. In this chapter a description of the model, debris flow material, debris flow breakers and the experimental plan and procedure will be given.

4.1   The Debris Flow Model

A scale model as used in this master thesis enables us to demonstrate the behaviour of a debris flow and debris flow breakers without examining the original object itself. The Debris Flow Model used in this master thesis was first built in 2009 for an assignment given by the Norwegian National Road Administration. The assignment was carried out by Hiller and Jensen (2009) where they investigated the effect of deflection structures to channel debris flows under a bridge. Figure 4.1 shows the model in

2009.

Figure 4.1: The debris flow model in 2009 when it was used to investigate the effect of channeling debris flows under a bridge by using deflection structures (Hiller and Jensen, 2009).

The model is a principle model with an approximate scale of 1:20. Using a principle model means that the model represents a typical debris flow event, not a specific event. The model is located at the Department of Hydraulic and Environmental Engineering at NTNU, but belongs to NPRA.

In 2012 the model was further developed when Fiskum (2012) used it to investigate the effectiveness of check dams, slit dams and baffles. He added a table where the debris flow could run out. This made it possible to study the runout distance and pattern. In 2013, when Christiansen (2013) investigated the effect of deflection struc-

tures and channels she expanded the run-out table even more. Figure 4.2 shows how the runout table looks today.
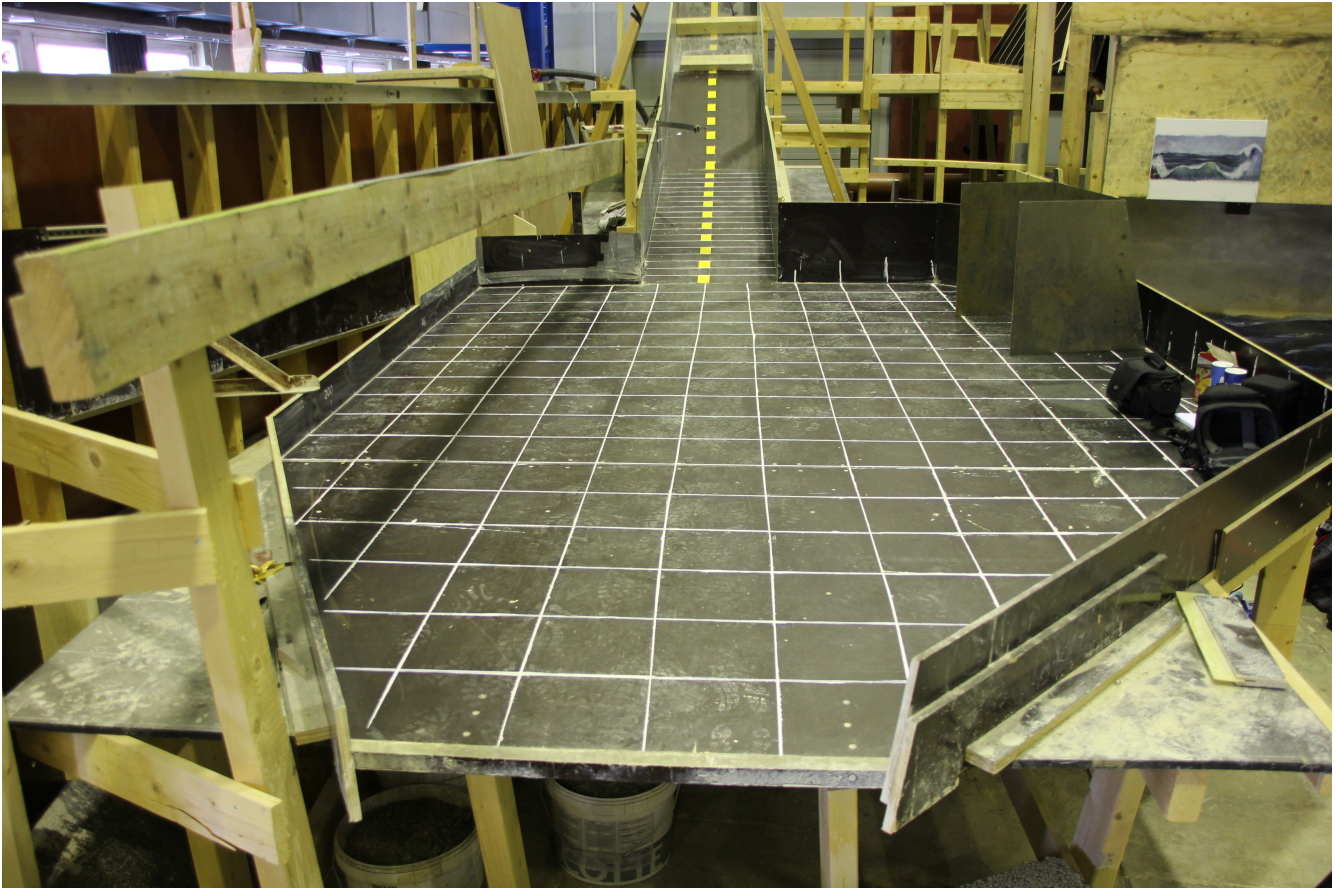
Figure 4.2: The runout table of the debris flow model after it was repainted. The table is 360 cm long and the grid is 20 x 20 cm.

The grid on the runout table and the lines in the channel needed to be repainted before the model could be used. During testing some of the lines were worn out, but these were repainted again.
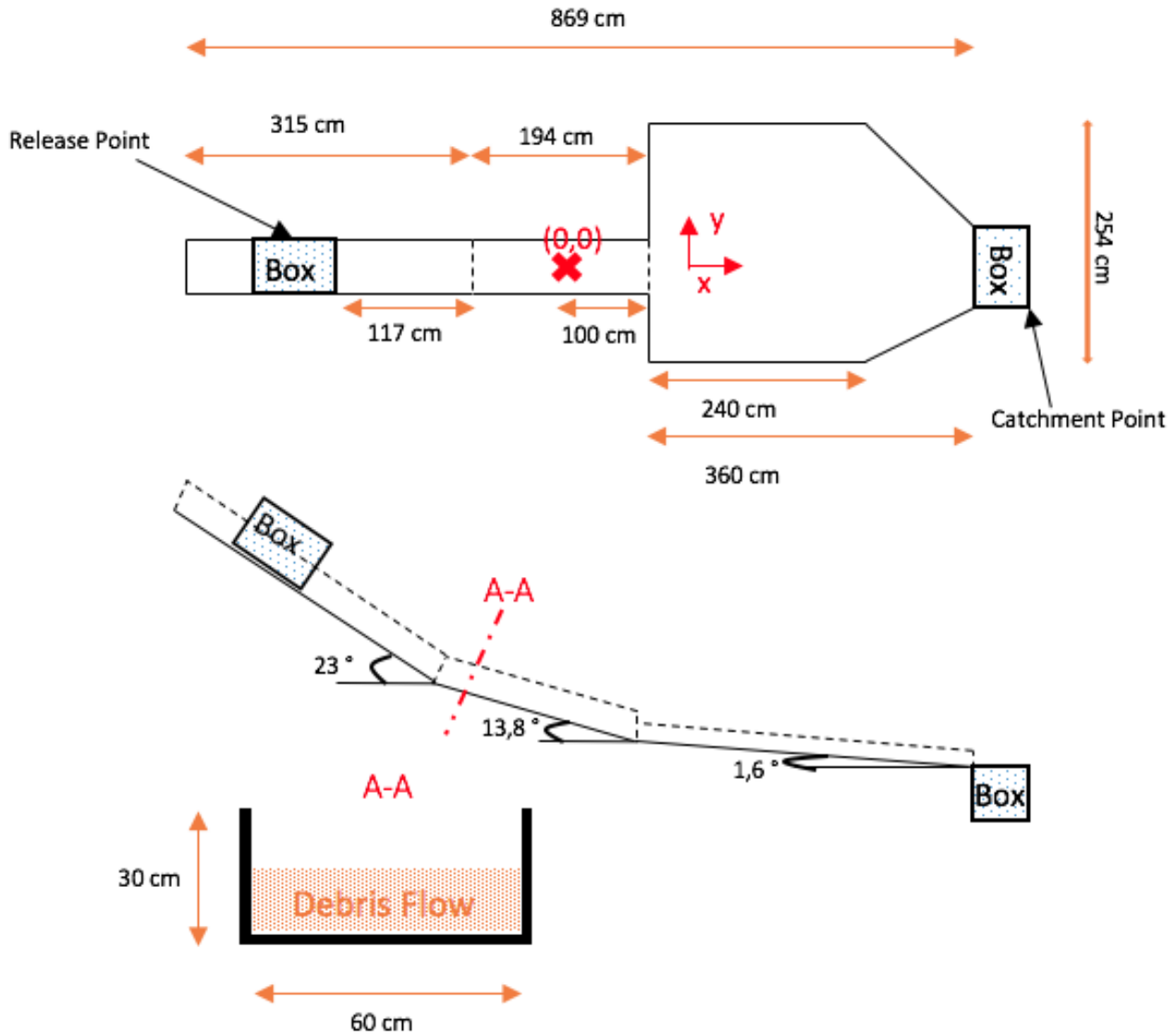
Figure 4.3: Illustration of the model seen from above and from the side. All the measurements are taken from Christiansen (2013). Adapted from Christiansen (2013)

4.1.1   Model Laws

In order to compare the results from the physical model to real debris flows simili-tude for all dimensionless quantities must be equal for both scaled model and the real prototype. The Froude number has been used by both Fiskum (2012) and Chris-

tiansen (2013) and is the most used model law for rapid mass movements. This number expresses the relationship between the gravitational forces and the inertia forces and should be approximately the same for the model and in nature. The Froude number is expressed as:

$$Fr = \frac{v}{\sqrt{gh}} \tag{4.1}$$

where

v = velcity of the debris flow [m/s]

g = acceleration due to gravity (9,81 [m/s^2])

h = flow height [m]

Debris flows in nature usually have a velocity between 5-10 m/s, and a height around 1 m (can be 3 m for very large debris flows). This gives a Froude number between 1.60-3.19.

The scale of the model is:

$$\lambda = \frac{model}{nature} = \frac{1}{20} \tag{4.2}$$

The Froude number can be used to compare or predict the velocity and flow height of a natural debris flow to the model experiments.

$$Fr_{model} = Fr_{nature}$$

$$\frac{v_{model}}{\sqrt{gh_{mmodel}}} = \frac{v_{nature}}{\sqrt{gh_{nature}}}$$

$$\frac{h_{nature}}{h_{model}} = \frac{v_{nature}^2}{v_{model}^2}$$

$$v_{model} = v_{nature} \cdot \sqrt{\lambda} \tag{4.3}$$

$$h_{model} = h_{nature} \cdot \lambda \tag{4.4}$$

Based on the velocity and flow height of real debris flows the expected values in the model becomes:

$$v_{model} = 5[m/s] \cdot \sqrt{\frac{1}{20}} = 1.12[m/s]$$

$$v_{model} = 10[m/s] \cdot \sqrt{\frac{1}{20}} = 2.24[m/s]$$

$$h_{model} = 1[m] \cdot \frac{1}{20} = 0.05[m]$$

4.2 Debris Flow Material

The material present in a debris flow is complex and may vary from clay sized solids to boulders of several meters in diameter. It is therefore no exact answer to what kind of material to be used when physically modeling a debris flow. For previous experiments carried out on the debris flow model at NTNU the same material was used for all tests. This is mostly due to the difficult release of the debris flow in the model. Both Fiskum (2012) and Christiansen (2013) tried to do test with different materials and combination of water and solids but they encountered problems when the debris flow did not easily flow out of the release box. Due to this and limited time it was decided to use the same material and combination of water and solids that was the most successful for Hiller and Jensen (2009), Fiskum (2012) and Christiansen (2013). However, there was little left of the material and no one knew exactly where it came from. One of the engineers working at the laboratory thought it might originate from Spain or Greece. Therefore, a new material had to be used. In order to avoid problems with the release it was decided to make a material as similar as possible to the material that had been used before. This would also allow for comparison of the countermeasures tested now and the ones that had been tested before. The new material was made out of the different material available at the Road laboratory at NTNU. Three kind of materials were sieved separately and in combinations to find the best fit. The NPRA sieving procedure was used to obtain the grain size distribution (GSD) curves for comparison. The different d values were also established to compare these and their deviations from the old material. The material available was:

1. 0-4 mm from Steinkjer

2. 0-8 mm from Steinkjer

3. 4-8 mm from Lauvåsen

The GSD curve of the old material is given in figure 4.4. From the three materials available at the road lab only the 0-8 mm material could be a good match. The GSD curve of this material is also given in figure 4.4.
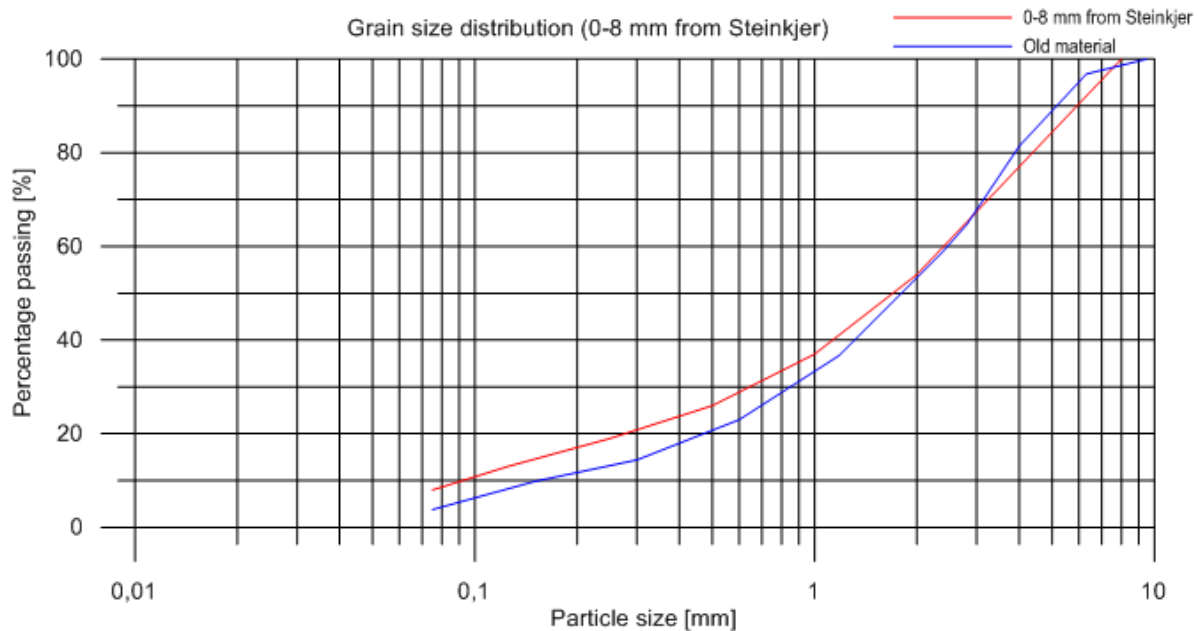
Figure 4.4: Grain size distribution curve of the old material (blue) and the 0-8 mm material from Steinkjer (red).

From these curves one can see that the 0-8 mm material was not so far off from the old material, but it had too much fine grains and too little coarse grains. To see if an even better match could be found, different combinations of the materials were sieved. Figure 4.5 shows all the grain size distribution curves of the tested combinations. The combinations that seemed to fit the best were sieved 3 times to make sure

that they all would get the same GSD curve.
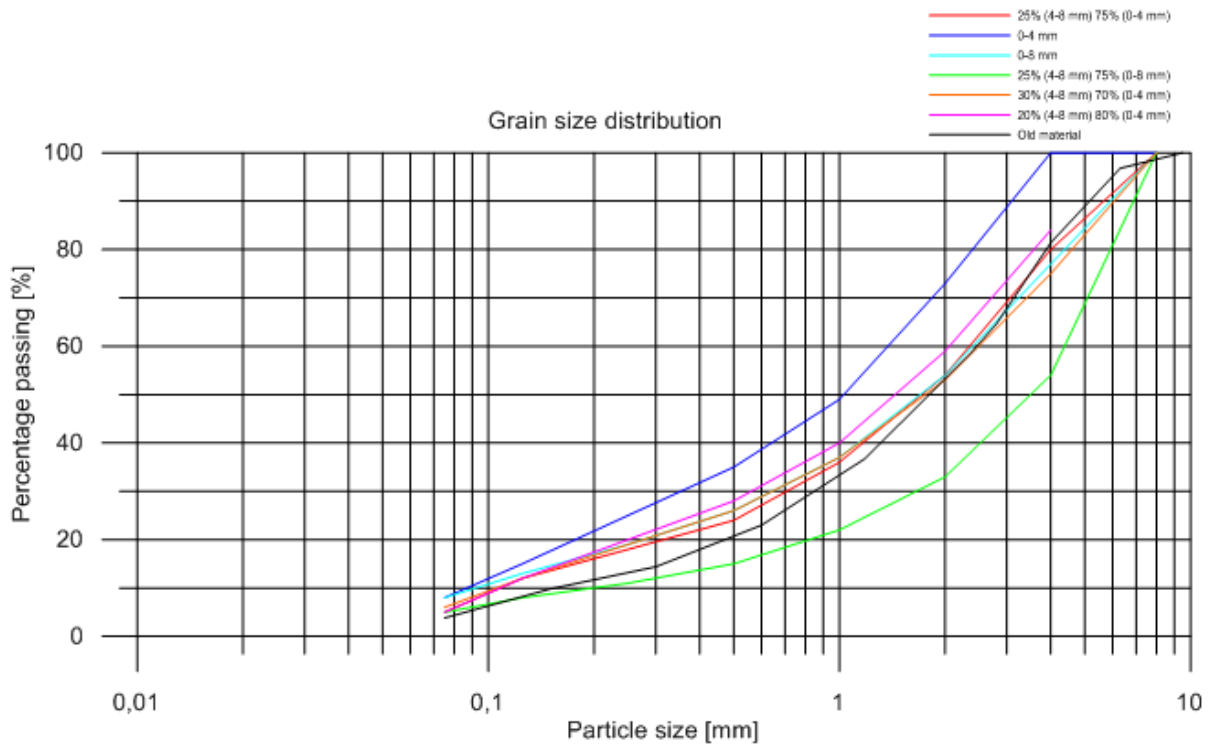
Figure 4.5: Grain size distribution curves for all the sieved materials and material combinations.

Even though the 0-8 mm material seemed to be a good fit, it was the combination of 25% 4-8 mm and 75% 0-4 mm that proved to be the best. The GSD curve of this combination can be seen in figure 4.6 where it is called the new material. The GSD curve of the old material used first by Hiller and Jensen (2009) is also in figure 4.6.
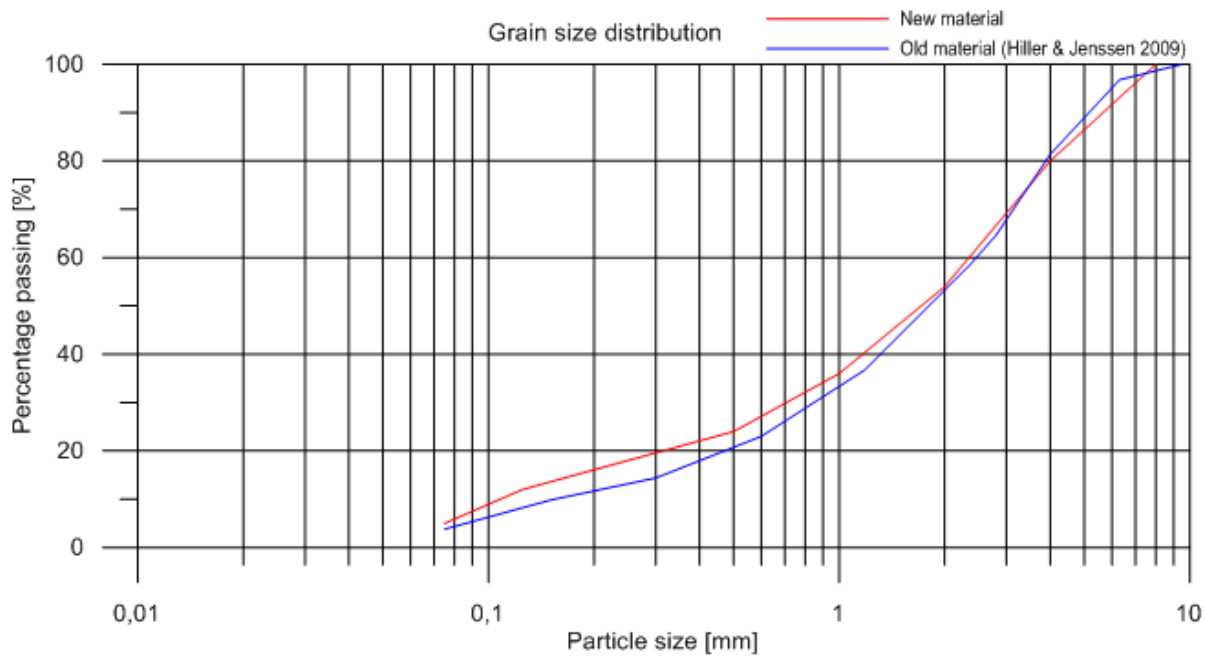
Figure 4.6: The grain size distribution curve of the debris flow material used for this master thesis (red) and for the material used in previous master thesis and experiments (orange).

The d_{values} of the new and old debris flow material is given in table 4.1. The dry density of the new material is 2.71 g/cm^3.

Table 4.1: The d_{values} for the old and new debris flow material.

d_value	d_10	d_20	d_30	d_40	d_50	d_60	d_70	d_80	d_90
New material	0.11	0.3	0.7	1.2	1.8	2.5	3	4	5.5
Old material	0.15	0.5	0.9	1.5	1.9	2.5	3	4	5

4.3 Debris Flow Breakers

In the physical experiments carried out by Gonda (2009) and Kim et al. (2012)) the debris flow breaker was integrated into the channel so that it had the same slope as the channel. Due to time and resources the channel could not be remodeled, so the breakers had to be implemented differently. The solution was to make the breakers

go horizontally out of the slope as this would not require remodeling of the chan-
nel. Frank Staeli, engineer at the Department of Civil and Transport Engineering,
designed and crafted the debris flow breakers. The breakers were made like a puzzle
with pieces consisting of flat bars, discs and rods as seen in figure 4.7.
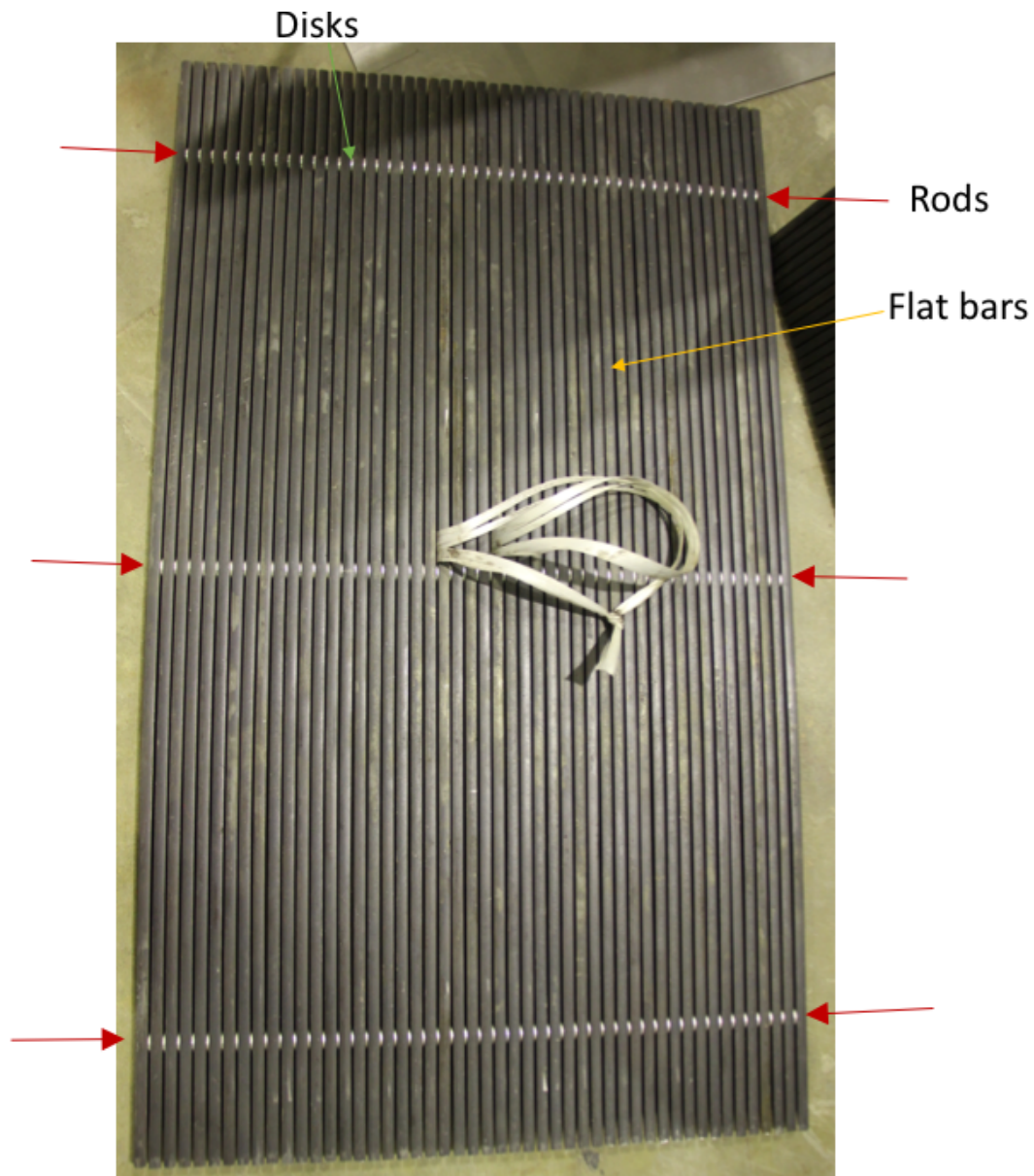
Figure 4.7: The 1.0 m long breaker with 2 mm opening width. The breaker has three rods keeping the
flat bars and discs together. There are 50 flat bars and 49 discs in this breaker. The white rope in the
picture was used to lift the breaker into the channel.

This design makes it possible to change the opening width of the breakers by placing discs in between each flat bar. The discs are 2 mm thick and one can vary the number of discs to change the opening width. The rods are there to keep the flat bars and discs together and are fastened by screws at each end. The process of rebuilding the breaker takes about 45 minutes as each flat bar and disc has to be cleaned before building a new breaker. Figure 4.8 shows the 0.5 m long breaker being built with a 6 mm opening width.

Figure 4.8: The 0.5 m long breaker leaning against a leca block while being built with 6 mm opening width.

Since the width of the breaker had to be 60 cm as the width of the channel, the parameters that had to be set for the debris flow breakers were the length and the opening- and blocking width. The blocking width was set to 10 mm as this was the thickness

of the flat bars. As a result, the opening width became the main parameter determining the percentage opening. Since Kim et al. (2012) had experienced the best results with the percentage opening being 36%, one opening was set to 6 mm which gave a 38% opening. In the light of the pore pressure theory presented in chapter 2 and the principle of debris flow breakers presented in chapter 3, it was decided that 2 mm openings should be tested to see if this was sufficient enough to drain out the water and decrease the pore fluid pressure present in the debris flow body. Also, to see if there was a linear relationship the third opening width was set to be 4 mm. This gave three different opening widths, 2, 4 and 6 mm which gave 17%, 29% and 38% opening. To see the effect of having the debris flow breaker going horizontally out of the channel, breakers with an opening width of 0 mm, solid plates, was tested. To test the length parameter it was decided to use a 0.5 and 1.0 m long breaker, in nature these would be 10 and 20 m long. This allows for interpretation of how long the debris flow has to flow over the breaker before the water starts to drain out and the pore fluid pressure start to decrease. Altogether, this gives 8 different debris flow breakers. Table 4.2 gives the name of each breaker and their parameters.

Table 4.2: The different debris flow breaker to be tested in the physical model and their parameters.

Name	Length	Width	Opening width	Blocking width	Percentage opening
0.5 m - 0 mm	0.5 m	600 mm	0 mm	10 mm	0 %
1.0 m - 0 mm	1.0 m	600 mm	0 mm	10 mm	0 %
0.5 m - 2 mm	0.5 m	600 mm	2 mm	10 mm	17 %
1.0 m - 2 mm	1.0 m	600 mm	2 mm	10 mm	17 %
0.5 m - 4 mm	0.5 m	600 mm	4 mm	10 mm	29 %
1.0 m - 4 mm	1.0 m	600 mm	4 mm	10 mm	29 %
0.5 m - 6 mm	0.5 m	600 mm	6 mm	10 mm	38 %
1.0 m - 6 mm	1.0 m	600 mm	6 mm	10 mm	38 %

Another interesting aspect considering the opening width of the breakers is how much of the material could potentially pass through them. This can be found by

looking at the GSD curve of the debris flow material and find the *d* value at the opening widths. Figure 4.9 shows the GSD curve of the material and the *d* value of the material for the 2, 4 and 6 mm openings. This shows that 54% of the material could pass through when the opening width is 2 mm, and 80% for 4 mm openings and 92% for the 6 mm openings which is almost all of the debris flow.
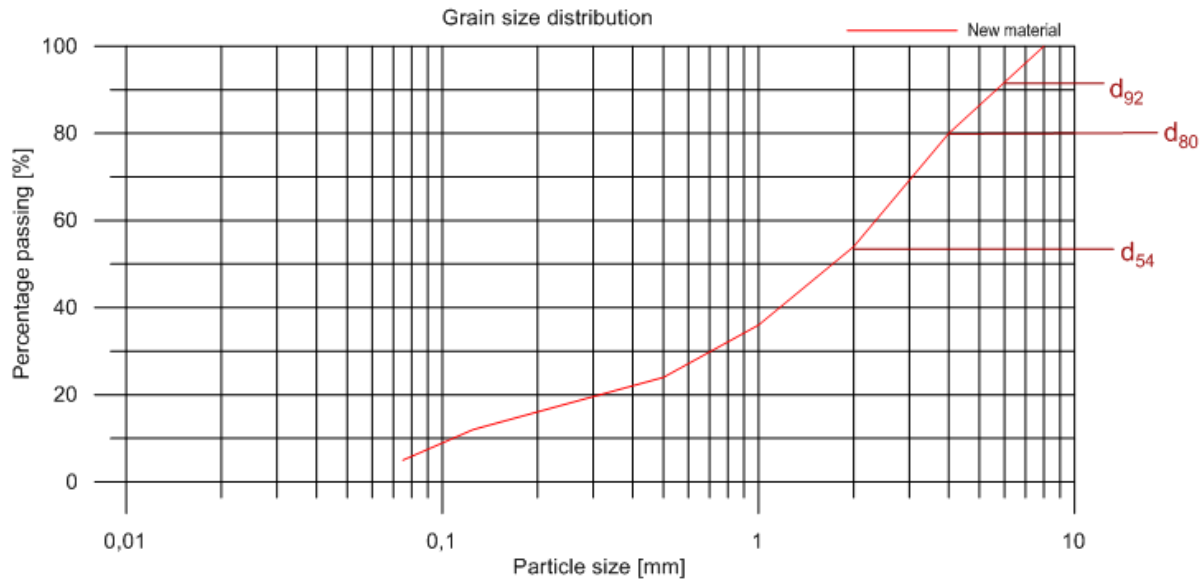
Figure 4.9: The GSD curve of the new material and the percentage of the material that can pass through the 2, 4 and 6 mm openings in the debris flow breakers.

4.4 Experimental Plan

Table 4.3 is an overview of all the planned tests and their parameters. Test 1-3 are the reference tests where there are no debris flow breakers in the channel. These tests are essential to have in order to compare the effect of the debris flow breakers in tests 4-27. However, since the debris flow breakers are built as a "jump" it is important to see the effect of the jump. Test 4-9 are therefore done with 0 mm opening widths, in other words a solid plate. The 0.5 m long solid plate can be seen in figure 4.10

and were also designed and crafted by Frank Staeli. A 1.0 m long solid plate was also made.

Table 4.3: List of all the planned tests and their parameters.

Test	Name	Length	Width	Opening width	Blocking width	Percentage opening
Test 1	Reference tests	-	-	-	-	-
Test 2						
Test 3						
Test 4	0.5 m - 0 mm	0.5 m	600 mm	0 mm	10 mm	0 %
Test 5						
Test 6						
Test 7	1.0 m - 0 mm	1.0 m	600 mm	0 mm	10 mm	0 %
Test 8						
Test 9						
Test 10	0.5 m - 2 mm	0.5 m	600 mm	2 mm	10 mm	17 %
Test 11						
Test 12						
Test 13	1.0 m - 2 mm	1.0 m	600 mm	2 mm	10 mm	17 %
Test 14						
Test 15						
Test 16	0.5 m - 6 mm	0.5 m	600 mm	6 mm	10 mm	38 %
Test 17						
Test 18						
Test 19	1.0 m - 6 mm	1.0 m	600 mm	6 mm	10 mm	38 %
Test 20						
Test 21						
Test 22	0.5 m - 4 mm	0.5 m	600 mm	4 mm	10 mm	29 %
Test 23						
Test 24						
Test 25	1.0 m - 4 mm	1.0 m	600 mm	4 mm	10 mm	29 %
Test 26						
Test 27						

Figure 4.10: The 0.5 m long solid plate which represents the debris flow breaker with 0 mm opening width. Two clamps are used to keep the structure in place. Duct tape is also used to create a smooth transition from the channel and onto the solid plate.

To compare the effectiveness of the debris flow breakers it was decided to only look at the runout and the energy lines. To make the energy lines one needed the flow velocity and the flow height of the debris flow. The velocity was obtained by analysing the videos afterwards and the flow height from the ultrasound sensors placed upstream and downstream of the debris flow breaker. Table 4.4 shows all the equipments used for the physical experiments while figure 4.11 illustrates where the equipments was placed.

Table 4.4: List of the equipment used in the physical experiments.

Equipment	Usage
Video camera 1	Films the whole model as a overview (25 frames per second (fps))
Video camera 2	To film upstream of the countermeasure and on the debris flow breaker (50 fps)
Video camera 3	To film downstream of the debris flow breaker (25 fps)
Video camera 4	To film the display of the ultrasound sensor (24 fps)
Ultrasound sensor	To measure the flow height of the debris flow before the countermeasure (13 updates per second)
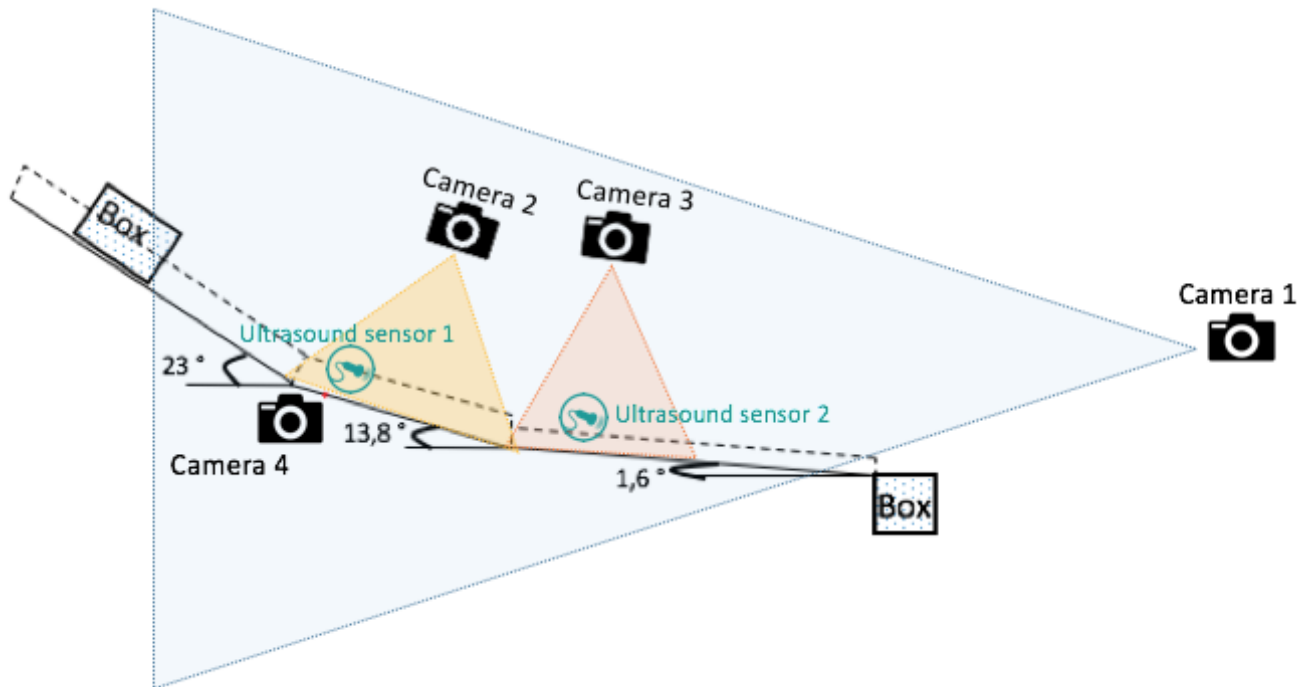
Figure 4.11: Illustration of the model profile and where the cameras and ultrasound sensors are placed. The triangles going out of the cameras represents the view from the cameras. Camera 4 does not have a triangle as this camera was only used to film the display of ultrasound sensor 1.

4.4.1 Test procedure

In order to check if the experiments were repeatable a test procedure was kept constant. Before any tests were carried out the weight of box A and B was registered in order to keep track of the weight of the debris flow material. For the first test one of

the boxes was filled with 80 kg of material and 20 kg of water, adding up to 100 kg of debris flow. Before and during a debris flow test this list had to be checked:

- Clean the model for water and sediment

- Weigh the box containing the debris flow and fill with water if there is some weight missing

- Lift the box containing the debris flow in place at the top of the model

- Check that the second box is closed and placed at the end of the model

- Place, focus and start the recording on all cameras

- Indicate which test by holding a paper with the test number in front of each camera

- Push the debris flow up against the box opening

- Use the mortar mixer to keep the suspension in the debris flow for approximately 15 seconds. The last rotations are done in the middle

- The release of the debris flow is to happen right after the the mortar mixer is pulled out of the box.

After a debris flow test this list had to be checked:

- Stop the recordings

- Take pictures of details that are not visible on the video recordings such as the remaining material in the box and runout

- Push all the debris flow into the box at the end of the table using a squeegee to collect all the water and small sediments

- Change the debris flow breaker if new conditions were to be tested next

- Weigh the box which the debris flow was released from and clean the openings to prevent leakage in the next test

The cleaning after a debris flow is time consuming and takes about 30-60 minutes depending on which countermeasures that was used and how many people working. Also, the personnel operating the crane was not always available so there was some downtime in between the tests. The 1 m long breakers were so heavy that it required a crane to lift them in place. This also made it difficult to clean under them after each test. To clean the breakers from a small plastic plate and dish brush was used to get the out the material clogged between the plat bars.

Chapter 5

Results and Analysis

This chapter presents the results from the 27 debris flow tests conducted at the Department of Hydraulic and Environmental Engineering at NTNU. The results include the debris flow front velocity, runout and flow height. The analysis includes GSD curves for material samples, energy lines and the effectiveness of the breakers in terms of reduced runout compared to the reference tests and the tests with the solid plates. There is no discussion in this chapter, only a presentation of the results.

5.1 Velocity

The velocity of the debris flow is measured by analysing the videos from each test. It is not possible to find the velocity of the whole debris flow mass, only the debris flow front. This was done by measuring the distance traveled over time by looking at each frame of the video.
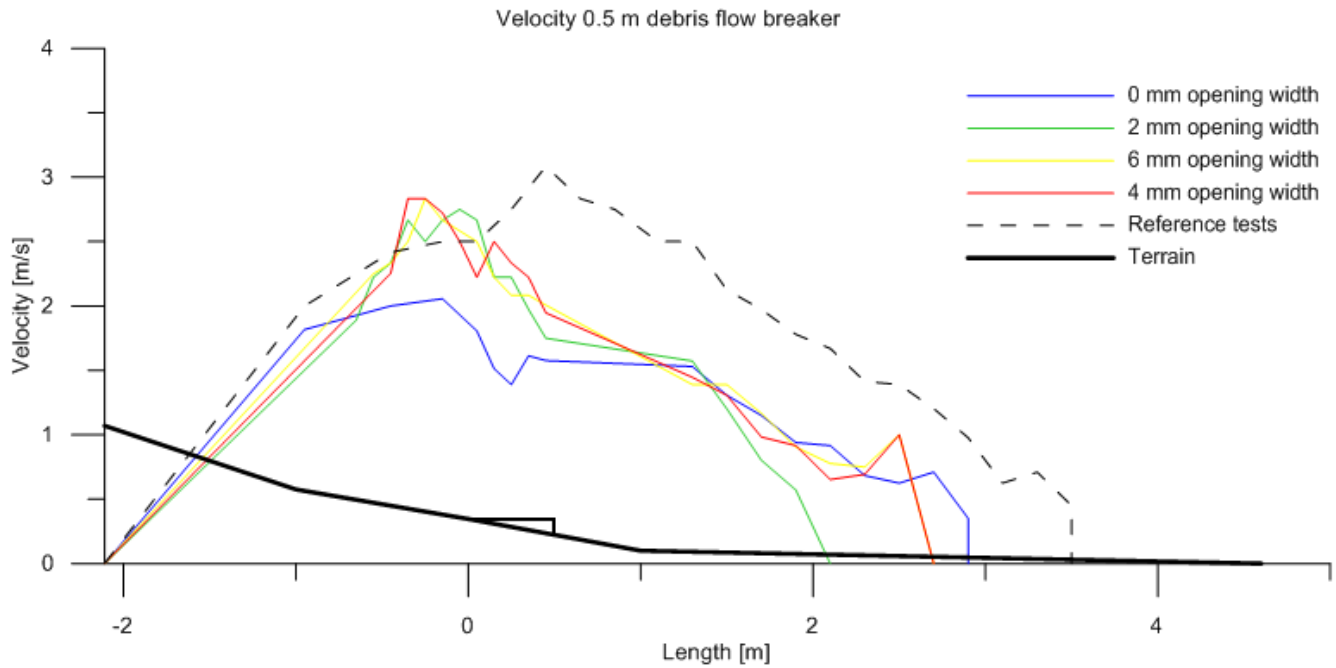
Figure 5.1: The debris flow front velocity of the 0.5 m long breaker with different opening widths. The reference test is the dash line each graph.
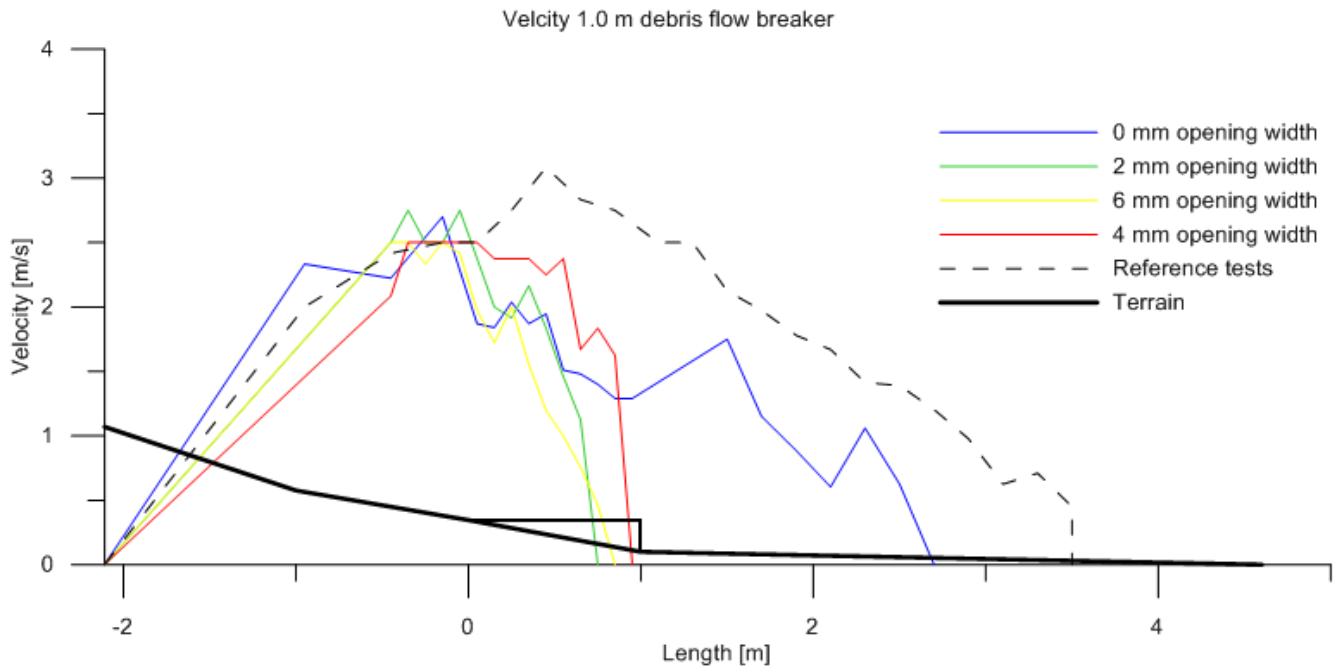
Figure 5.2: The debris flow front velocity of the 1.0 m long breaker with different opening widths. The reference test is the dash line each graph.

Figure 5.1 shows the velocity of the debris flow front for the average test for the 0.5

m long breaker while figure 5.2 is for velocity the 1.0 m long breakers. The dash line is the average reference test while the black line is the terrain of the model and the debris flow breaker.

5.2 Runout

The runout distance was measured in the flow direction from point 0,0 which is marked by the red "X" in figure 5.3 and figure 4.11. Table 5.1 gives the runout distance of all 27 tests and the effectiveness of the different breakers in terms of reduced runout distance compared to the reference tests and the tests with the solid plates.
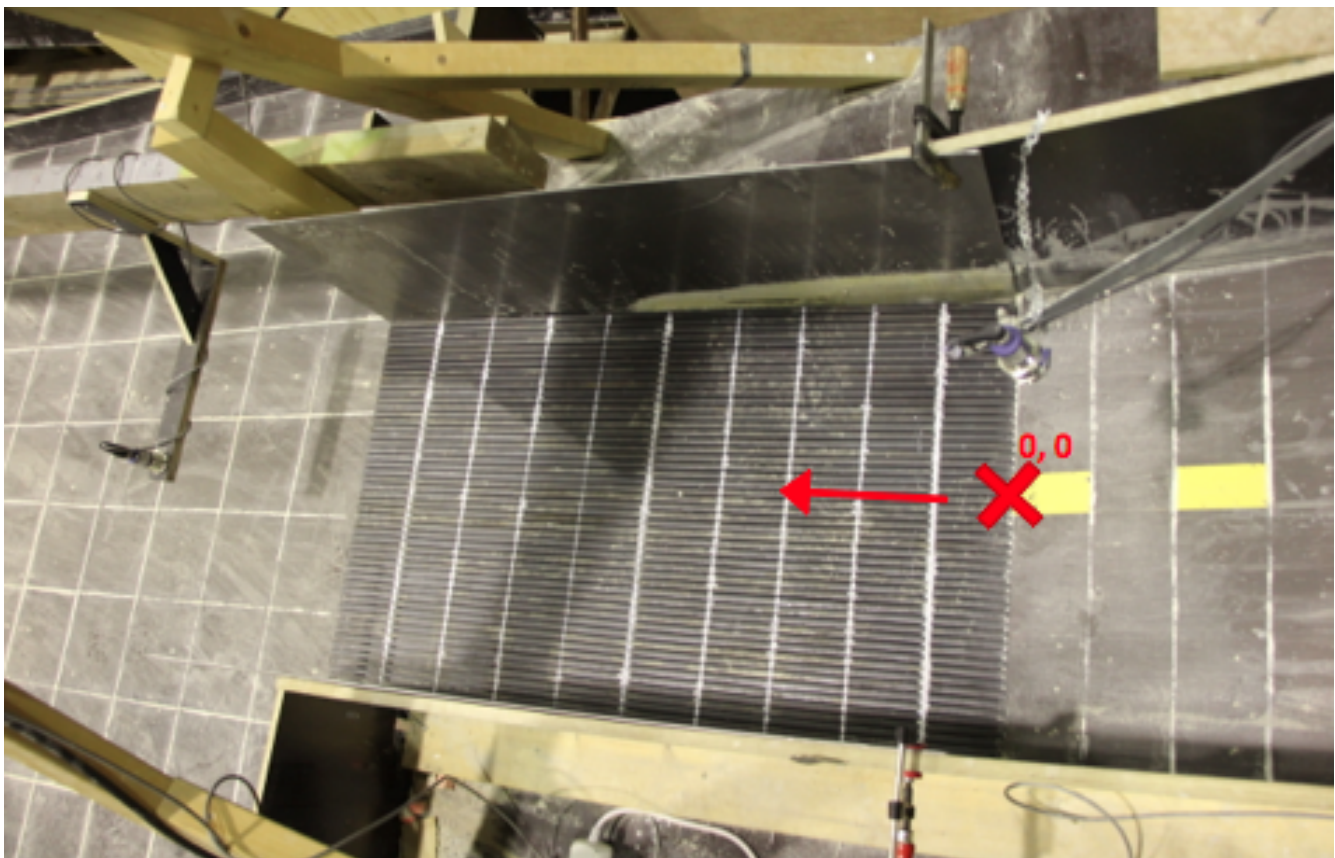
Figure 5.3: Point "X" indicates where the runout distance is measured from in the physical model. The red arrow shows the flow direction.

Table 5.1: The runout distance for all the tests, and the average runout distance for each condition/breaker. The effectiveness is measured in terms of reduced runout distance compared to the reference tests and the breakers with 0 mm opening width.

Test	Name	Runout distance [cm]	Average runout [cm]	Standard deviation [cm]	Effectiveness compared to the reference tests	Effectiveness compared to the 0 mm openings
1		330				
2	Reference tests	365	340	22	-	-
3		325				
4		240				
5	0.5 m - 0 mm	255	267	34	22 %	-
6		305				
7		265				
8	1.0 m - 0 mm	275	250	35	26%	-
9		210				
10		195				
11	0.5 m - 2 mm	180	200	23	41 %	25 %
12		225				
13		80				
14	1.0 - 2 mm	85	82	3	76 %	68 %
15		80				
16		240				
17	0.5 - 6 mm	300	263	32	23 %	1 %
18		250				
19		90				
20	1.0 - 6 mm	85	87	3	75 %	66 %
21		85				
22		220				
23	0.5 m - 4 mm	240	252	39	26 %	6 %
24		295				
25		75				
26	1.0 m - 4 mm	100	92	14	73 %	64 %
27		100				

Figure 5.4 shows a graphical presentation of the runout distance of the different openings in the debris flow breaker. The dotted horizontal line at 340 cm is the average runout for the reference tests.
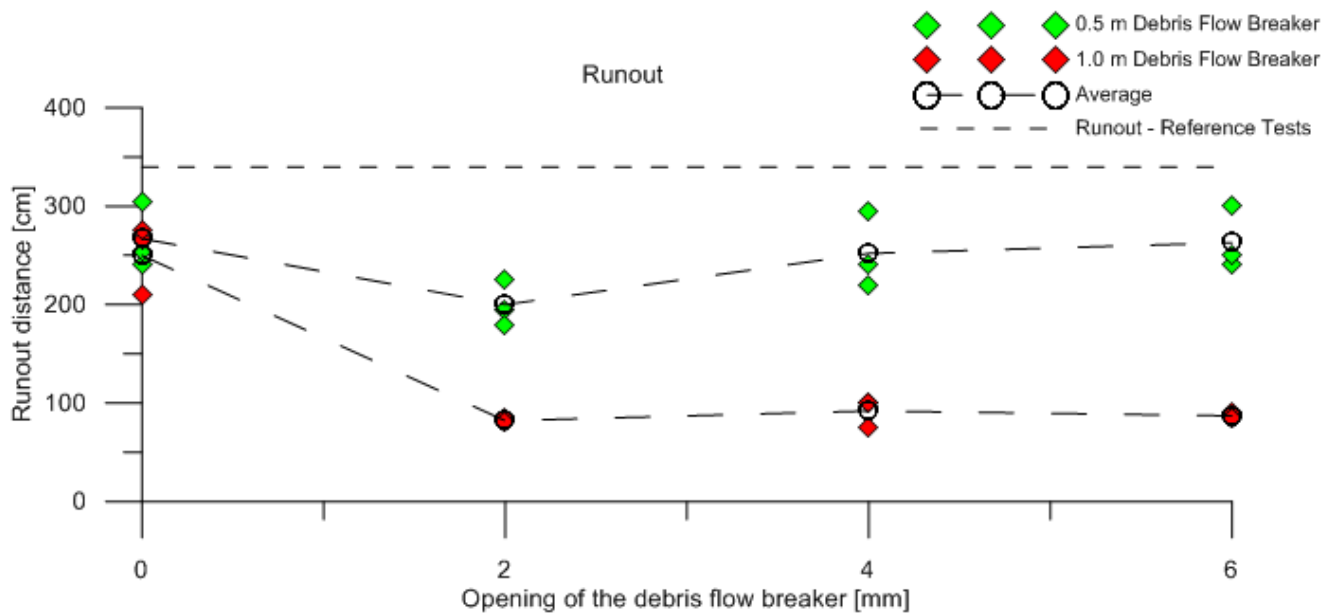
Figure 5.4: Variation in the runout distance with change in the opening width of the debris flow breaker.

After the debris flow stops water seeps out and continues to flow as a after flow down the runout table. However, when determining the runout distance and runout pattern it was decided to only look at where the debris flow first stopped, and not where the after flow stops. Figure 5.5 from test 9 shows this boundary which is indicated by the red line. When the 1.0 m debris flow breakers were tested the after flow was larger than the one from the reference tests and the 0.5 m long breaker. In these flows there were also very fine sediments that had passed through the opening widths of the breaker. Figure 5.6 shows the after flow that forms under the 1.0 m long breaker with the 2 mm opening width and where the debris flow front stopped on the breaker. Also for these cases it was decided to use the runout of the debris flow front, and not the runout of the after flow. One reason for not considering the runout of the after flow is that this flow does not hold the same destructive powers as the debris flow front. One example is if the after flow were to flow over a road, the drainage system of the road would most probably handle the watery after flow. However, if the debris

flow front were to hit the road it would cause large damages.
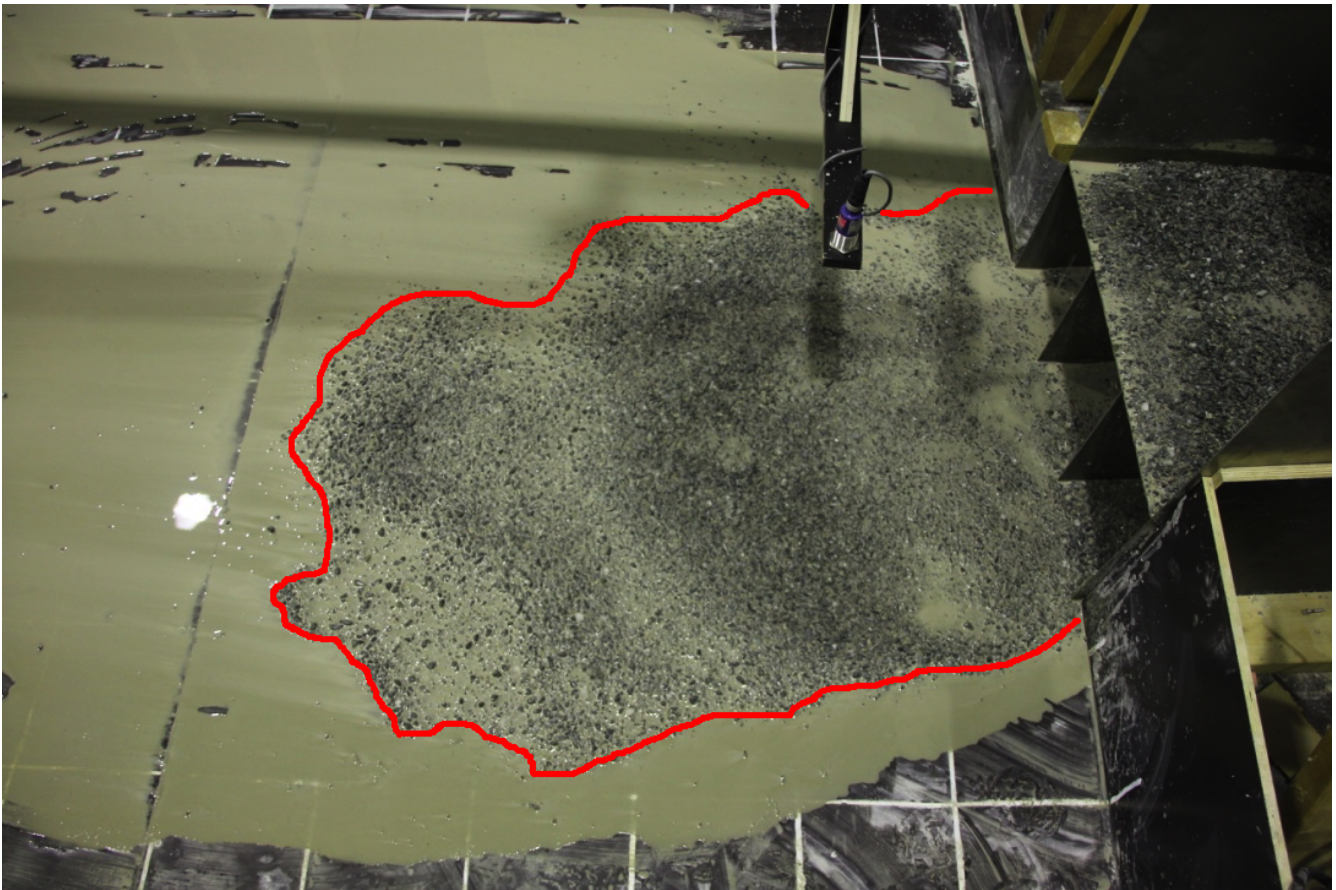
Figure 5.5: The red line indicates where the debris flow runout distance and pattern for test 9.
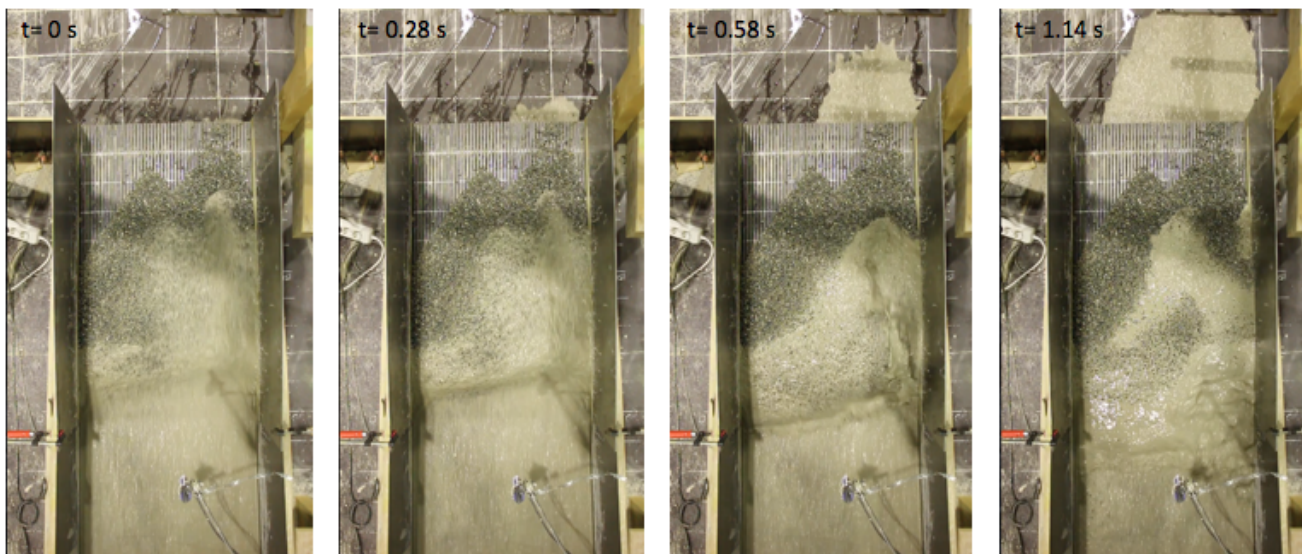
Figure 5.6: Video frames from test 14, 1.0 m long breaker with 2 mm openings. The debris flow front stops on the debris flow breaker. but a after flow forms of the water and fine sediments that drains through the debris flow openings.

To document the runout and runout pattern pictures were taken of each debris flow test. This was to compare and see if there were any major differences in how the debris flow runout appeared on the table. Figure 5.7 shows the runout for test 1-9 which are the reference tests and tests with the 0.5 m and 1.0 m solid plates.
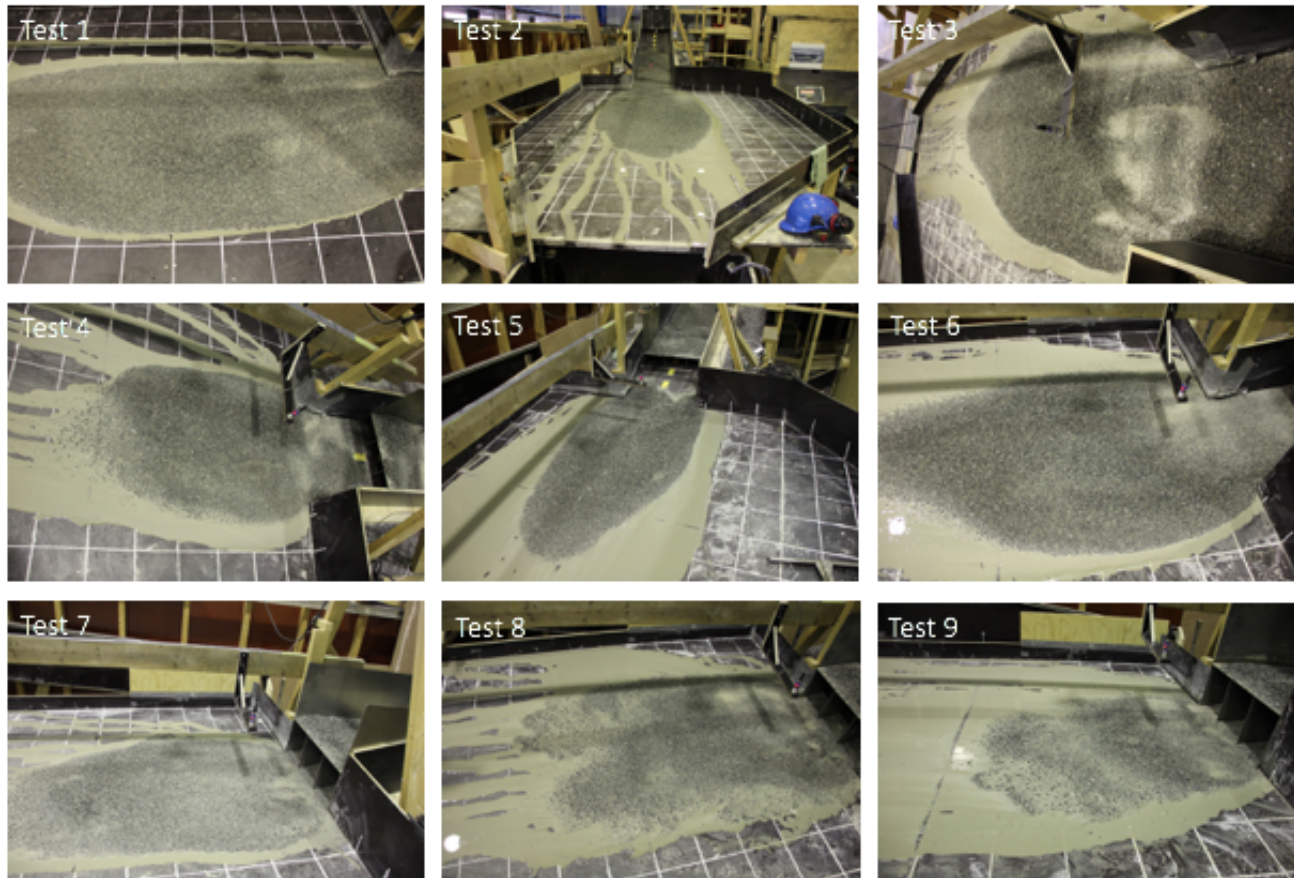
Figure 5.7: The runout of test 1-9. Test 1-3 is the reference tests, test 4-6 is the 0.5 m long solid plate and test 7-9 is the 1.0 m solid plate.

Figure 5.8 shows the runout for test 10-12 and 13-15 which are the tests with 2 mm openings for the 0.5 and 1.0 m long breaker.
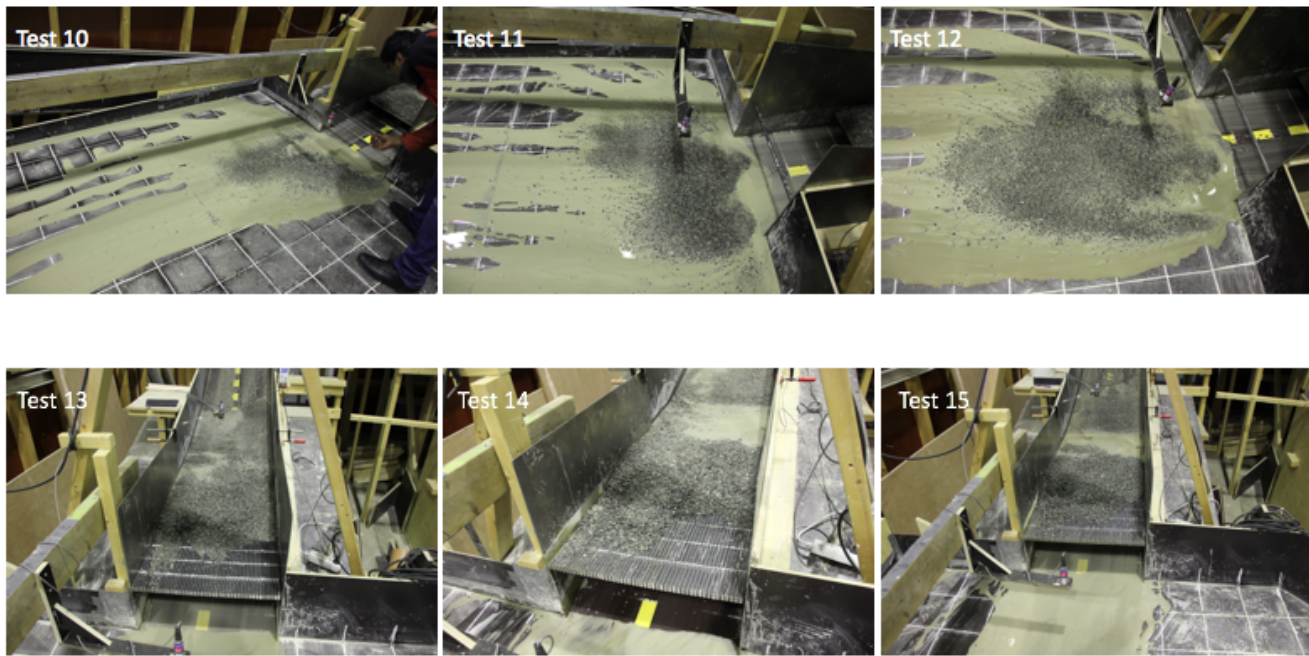
Figure 5.8

Figure 5.9 shows the runout for tests 16-21 when the opening width of the debris flow breakers was 6 mm. The pictures from test 21 were lost.
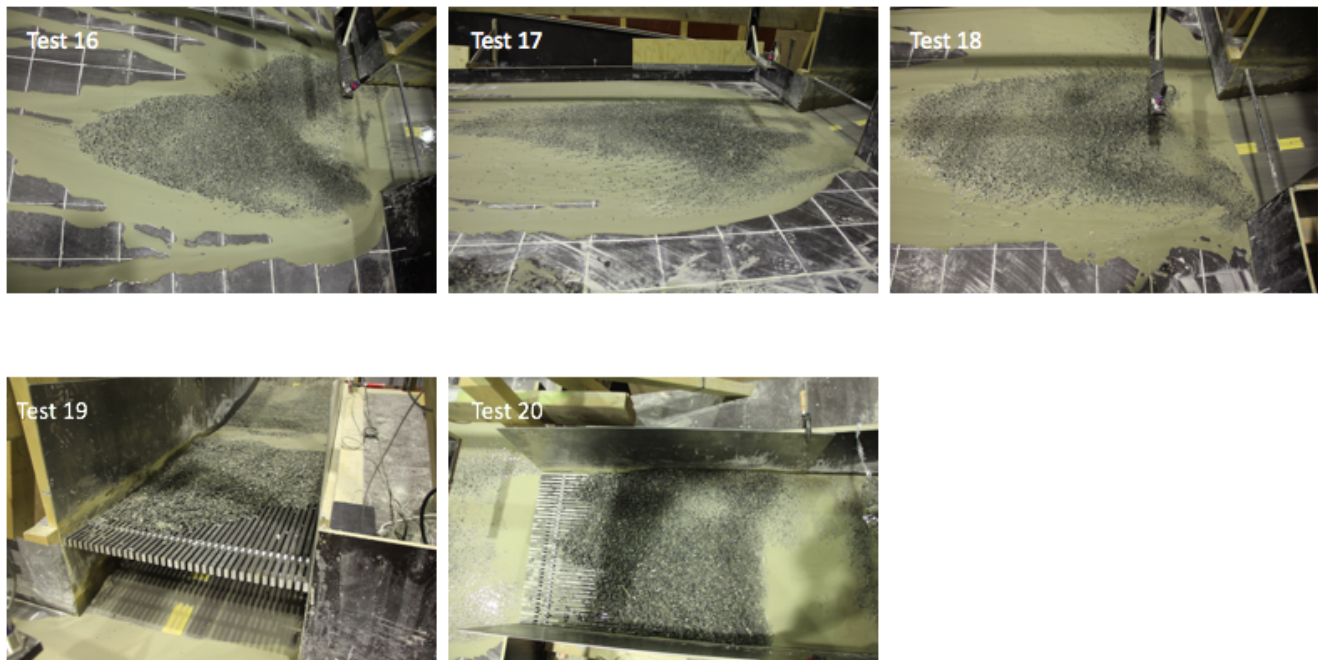
Figure 5.9: The runout for test 16-21. Test 16-18 is the 0.5 m long breaker with 6 mm opening width. Test 19-21 is the 1.0 m long breaker with 6 mm opening width. The picture of test 21 was lost.

Figure 5.10 shows the runout for test 22-24 and 25-27 which are the tests with 4 mm openings for the 0.5 and 1.0 m long breaker.
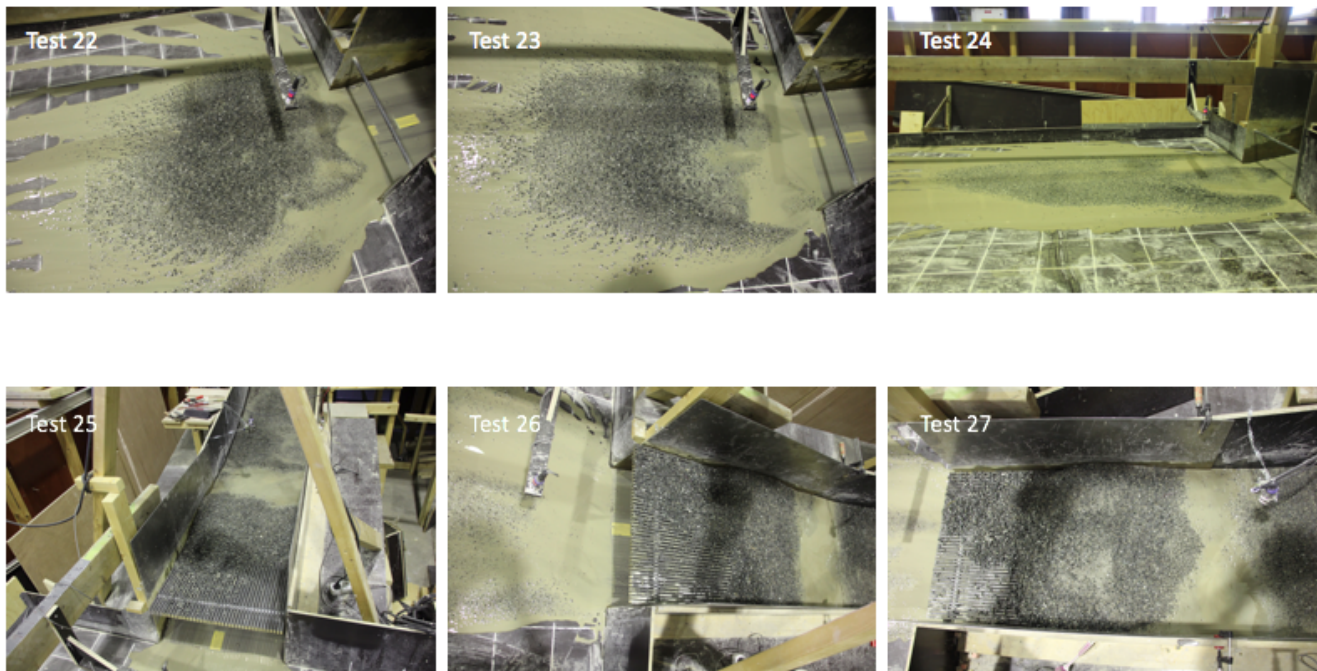
Figure 5.10: The runout for test 22-27. Test 22-24 is the 0.5 m long breaker with 4 mm opening width. Test 25-27 is the 1.0 m long breaker with 4 mm opening width.

Table 5.2 shows the reduced runout achieved by the different countermeasures tested by Fiskum (2012). These countermeasures included check dams, slit dams and baffles, alone or in combination. The reduced runout varied between 33% to 67%, where the check dam was the most effective.

Table 5.2: The effectiveness of the different countermeasures tested by Fiskum (2012) in terms of reduced runout compared to his reference tests.

Countermeasure	Effectiveness compared to reference tests
Check dam	67%
Slit dam - 2 slits	31%
Slit dam - 4 slits	42%
Baffles	14%
Baffles and slit dam (2 + 4)	44%
Baffles and slit dam (4 + 4)	40%
Baffles and wings	33%

For the countermeasures tested by Christiansen (2013) it was not possible to find the reduced runout distance. She tested deflection structures and channels which does not work the same way as the debris flow breakers or any of the countermeasures tested by Fiskum (2012).

5.3   Flow Height

The original plan included two ultrasound sensors to log the flow height upstream and downstream of the debris flow breakers. However, a computer was needed for this and at the time it was not available. Instead a camera was used to film the display of the sensor and then the flow height was registered by looking at each frame of the video (24 fps). Figure 5.11 shows the display of the ultrasound sensor placed upstream of the debris flow breaker. Unfortunately there was only enough cameras to film the upstream sensor, and not the downstream. However, the downstream flow height was registered at the end of each debris flow. Figure 5.13 and 5.14 shows the flow height upstream for the average test for the different 0.5 m and 1.0 m long breakers and table 5.3 gives the flow height downstream of the breaker. Both the upstream and downstream flow height gives an indication of how much debris flow deposited upstream and downstream of the breakers. The upstream flow height of the reference tests also gives a profile of the debris flow, this is seen in figure 6.3 which is the flow height for test 1-3.

Figure 5.11: The display of the ultrasound sensor placed upstream of the debris flow breaker in the center of the channel at x= -115.
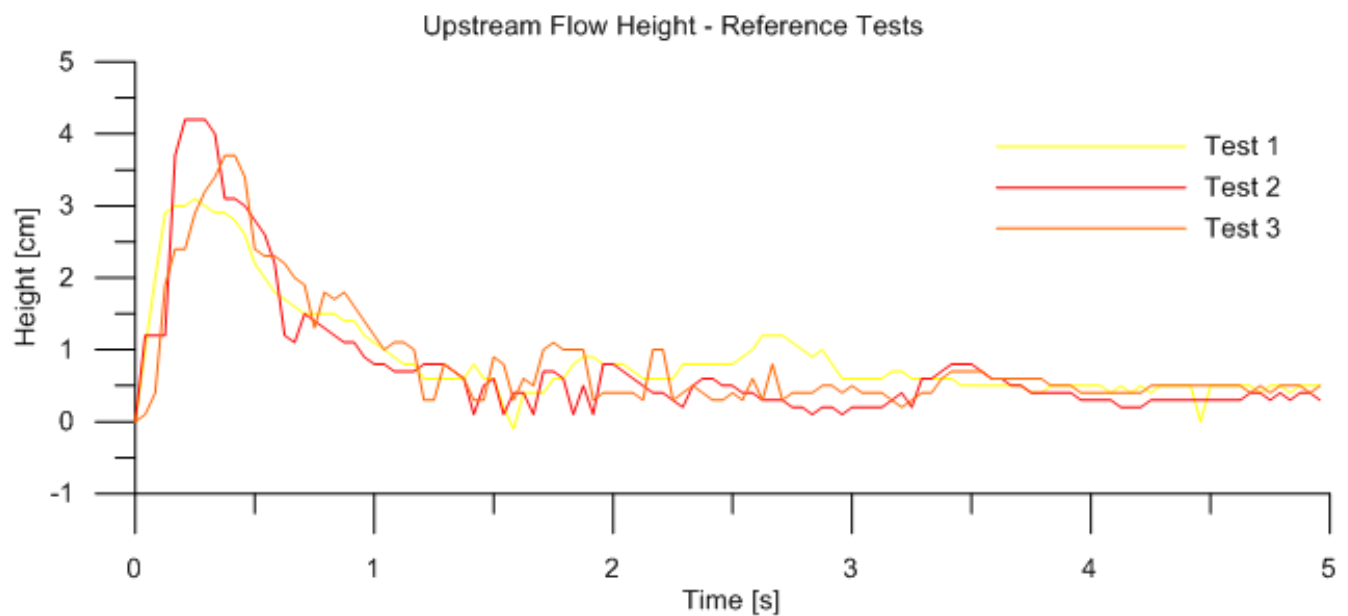
Figure 5.12: The flow height upstream of the reference tests 1-3 over a 5 second time period.
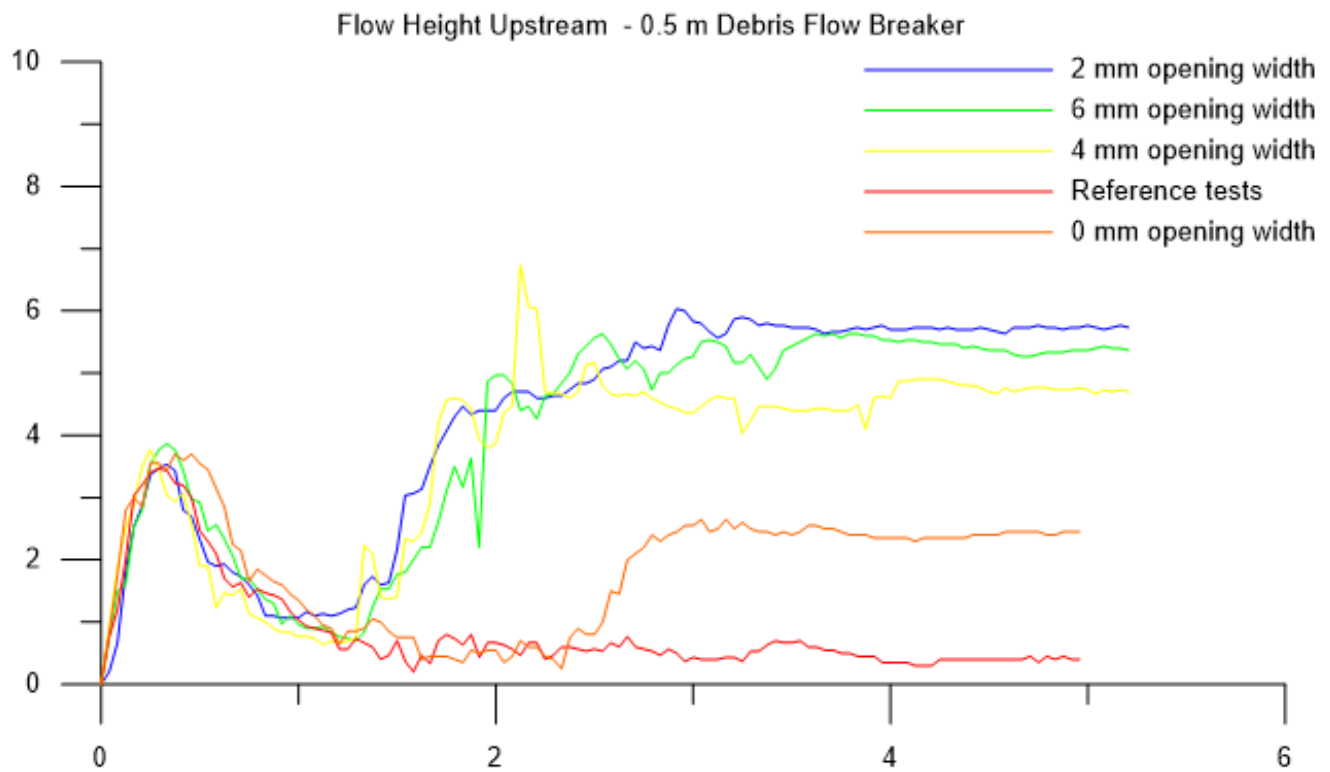
Figure 5.13: The flow height of the average debris flows of the different 0.5 m long breakers, and the flow height of the average reference test.
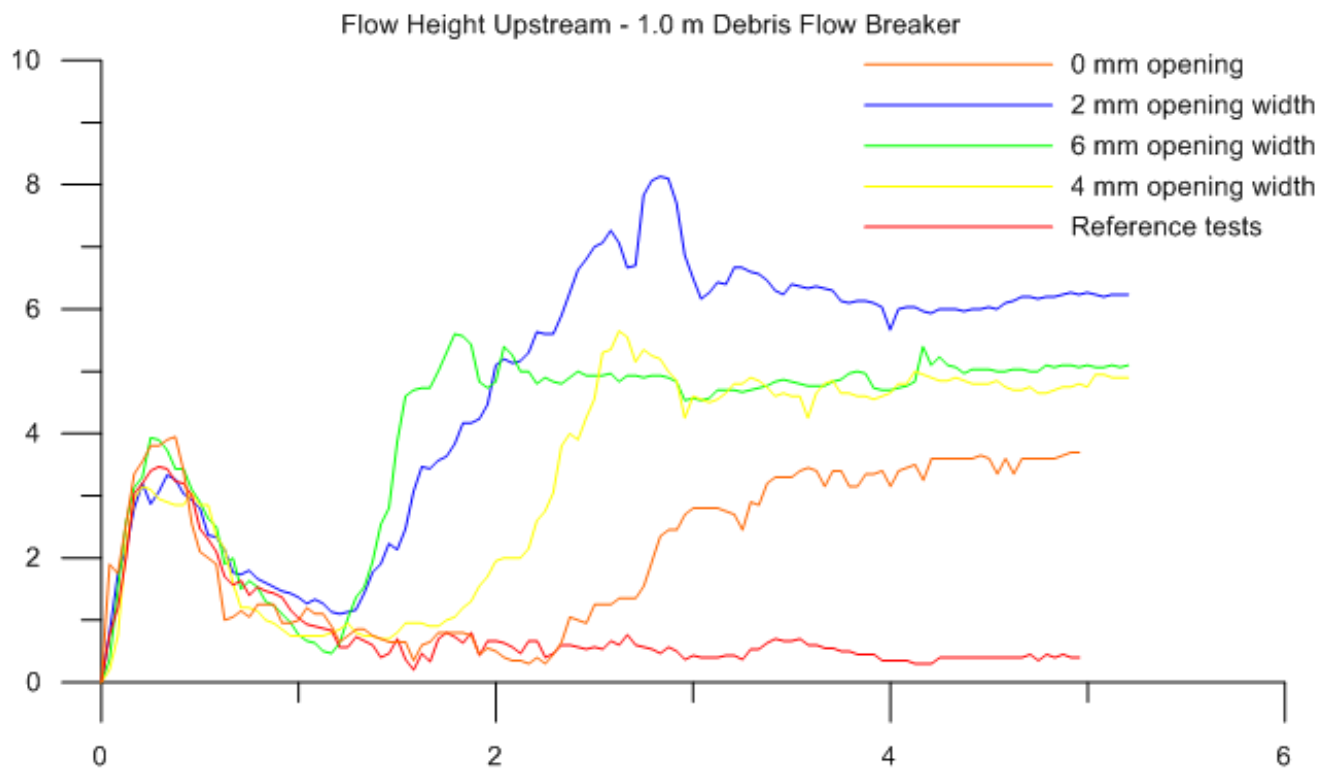
Figure 5.14: The flow height of the average debris flows of the different 1.0 m long breakers, and the flow height of the average reference test.

Table 5.3 shows the average deposition height of the stopped debris flow upstream and downstream of the debris flow breaker.

Table 5.3: Average slope of the running average trend line of the energy line upstream and downstream of the debris flow breakers.

Condition	Deposition height upstream [cm]	Deposition height downstream [cm]
Reference tests	0.4	1.5
0.5 m - 0 mm	2.45	1.7
1.0 m - 0 mm	3.7	1.1
0.5 m - 2 mm	5.73	1.3
1.0 m - 2 mm	6.2	0.5
0.5 m - 4 mm	4.7	1.2
1.0 m - 4 mm	4.9	0.8
0.5 m - 6 mm	5.37	1.8
1.0 m - 6 mm	5.1	0.5

5.3.1 Material Samples

Material samples were collected upstream and downstream of the 0.5 m long debris flow breakers for test 10, 16 and 24. This material was sieved to obtain the SD curves which gives an indication of what material was keep upstream and what material drained through or flowed over the breakers. Figure 5.15 shows the GSD curves of the samples for the 0.5 m long breakers with 2, 4 and 6 mm openings. The upstream samples were collected from the debris flow breaker as indicated in figure 5.16 while the downstream samples were collected from the runout table.
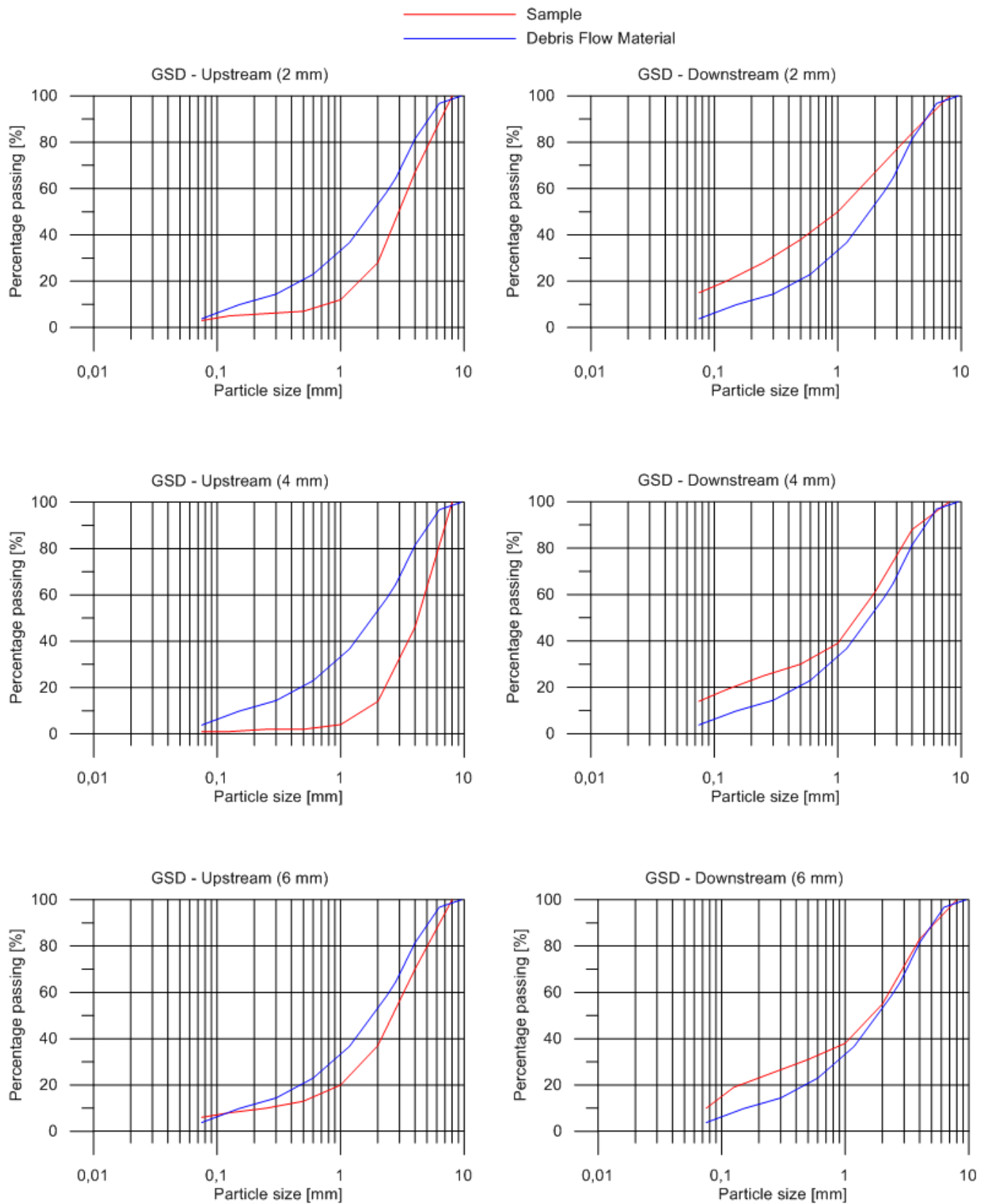
Figure 5.15: The different GSD curves of the material samples collected upstream and downstream for the debris flow breakers for tests 10, 16 and 24. Test 10 is the 2 mm opening, test 16 the 6 mm opening and test 24 is the 4 mm opening.

Figure 5.16: The material sample is collected from the front of the debris flow where the arrow is pointing.

5.4 Energy lines

The energy lines for the different opening widths for the 0.5 m and 1.0 m long breaker are given in figure 5.17 and 5.18 together with the energy line of the average reference test. Due to the uneven energy lines a trend line of the running average is added to each one. The slopes of the trend line upstream and downstream of the breakers are given in table 5.4 and the energy line and trend line of the average test for each condition are given in appendix **??**.
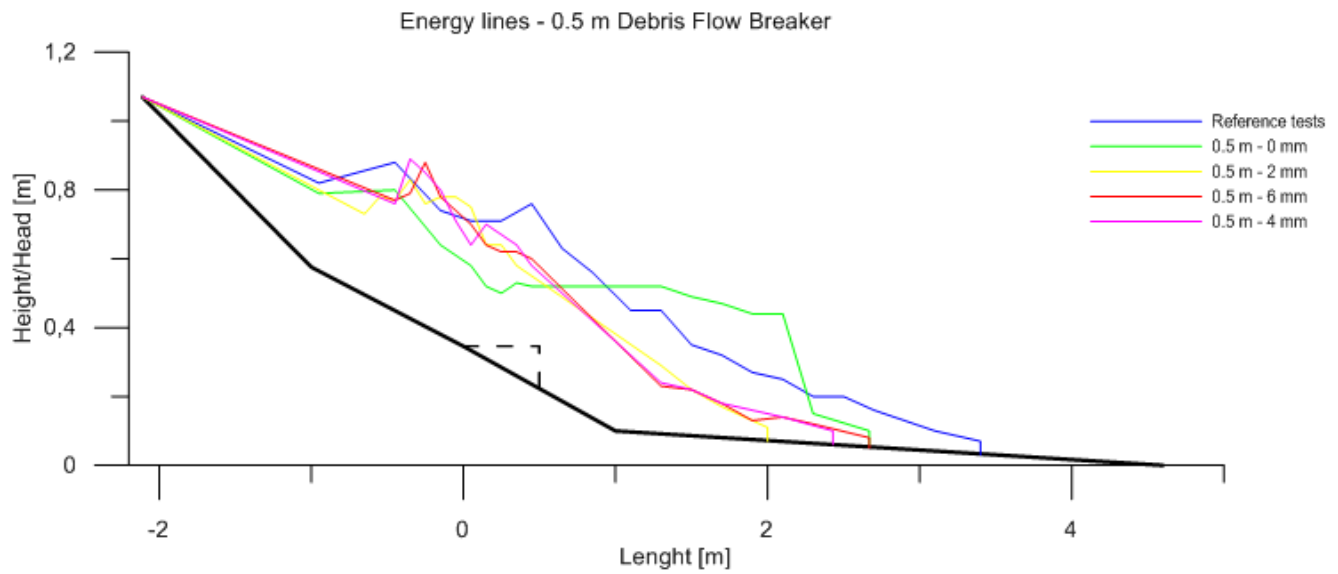
Figure 5.17: Energy line for the average test for all the 0.5 m long breakers and the solid plate.
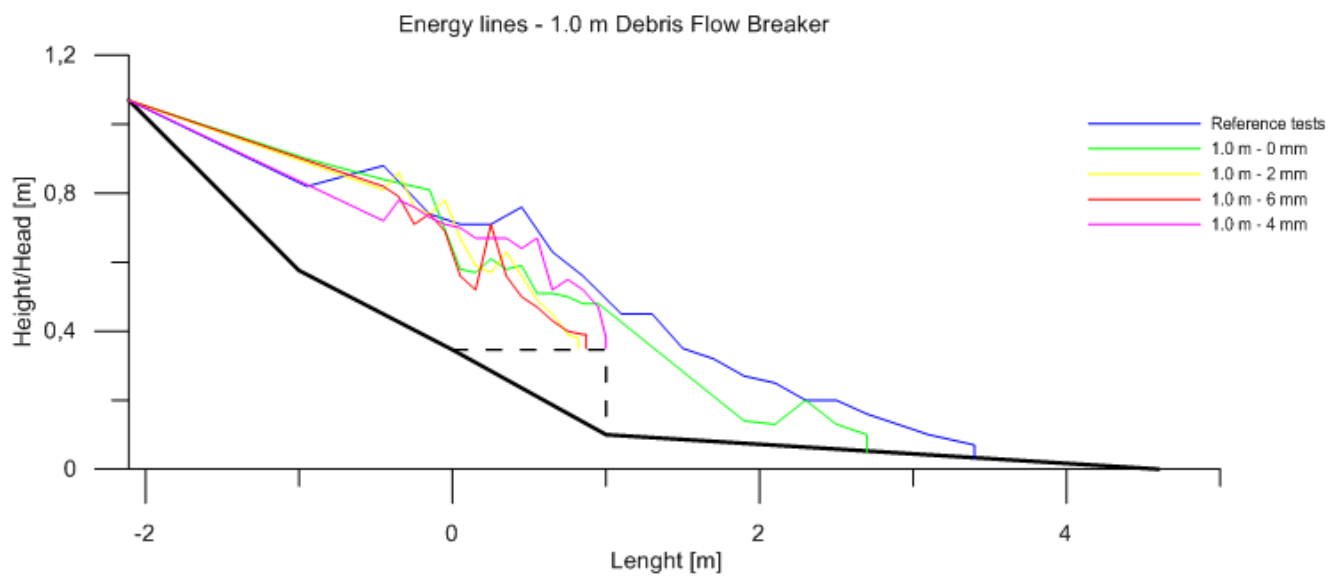
Figure 5.18: Energy line for the average test for all the 1.0 m long breakers and the solid plate.

Table 5.4: The average slope of the running average trend line of the energy lines upstream and downstream of the debris flow breakers. For the 1.0 m long breakers there was no debris flow downstream of the break with the exception of the breaker who had 0 mm opening.

Debris flow breaker	Average slope of the trend line	
	Upstream	Downstream
0.5 m - 0 mm	0.31	0.34
1.0 m - 0 mm	0.28	0.24
0.5 m - 2 mm	0.19	0.49
1.0 m - 2 mm	0.42	-
0.5 m - 4 mm	0.44	0.33
1.0 m - 4 mm	0.40	-
0.5 m - 6 mm	0.40	0.27
1.0 m - 6 mm	0.60	-

Chapter 6

Discussion

In this chapter the results and analysis will be examined and discussed in the light of the objectives of this work. First, the physical modeling of the debris flow will be discussed, this is the reference tests and then the debris flow breakers. The topics addressed for the reference test are velocity, flow height and energy lines. For the breakers the discussion will in the light of the objectives stated in Chapter 1 related to the debris flow breakers.

6.1 Physical Modeling of the Debris Flow

To evaluate the physical modeling of the debris flow one can look at the reference tests to see if what is observed in these tests correspond to what is expected for this modeled debris flow. The parameters and results that can be compared to a real debris flow is the velocity, runout, flow height and the energy lines. However, no prediction was done for the runout so this will not be discussed in the same manner

as the other parameter.

6.1.1 Velocity

From section 4.1.1 the expected velocity of the debris flow in the model was 1.12-2.24 m/s. This was calculated from the model laws using the Froude number. Figure 6.1 shows the velocity of the debris flow front of the average reference test.
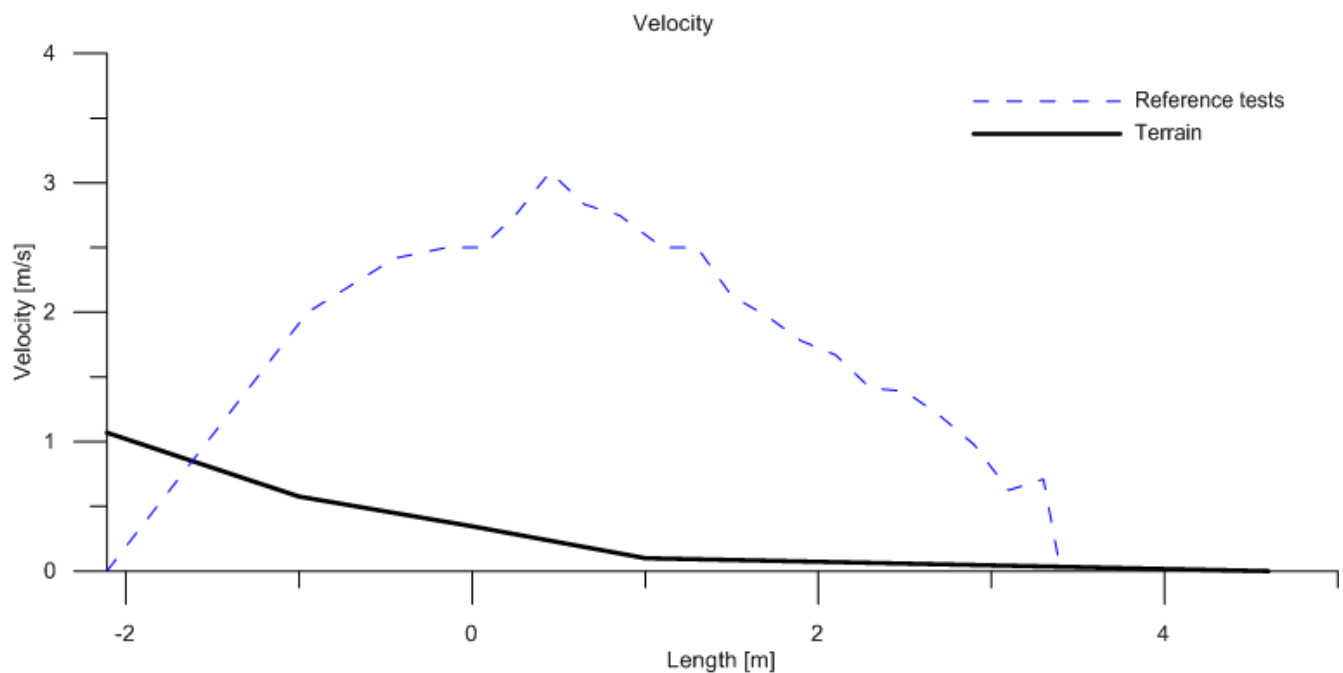
Figure 6.1: The velocity over the model length of the average reference test.

The maximum velocity reached was 3.08 m/s which is higher than the expected value. For a real debris flow this would equal 13.8 m/s which is fast for a debris flow. Whereas the average velocity down the channel was 2.31 m/s which is more like the expected velocity but still in the upper bound. The maximum velocity was reached at x= 0.45 m which is in the 13.9 ° slope. It is believed that the slope has to be steeper than 16 ° for a debris flow initialize, this indicates that in this part of the channel the debris

flow should start to slow down which is does after x= 0.45 m. There is also a peak right before the debris flow stops. This is probably due to problems interpreting the velocity as this procedure involved measuring the time the debris flow front used to travel a certain length by looking at each frame of the videos. However, the debris flow front often changed shape as some parts of the flow had larger velocities than other parts. Trying to keep the interpretation constant, the velocity was measured along the center line although this was not always where the front of the debris flow front was.

Figure 6.2 shows four different frames from the upstream video camera for test 2. Here it is possible to see that it was not the front of the debris flow front This illustrated that the debris flow front has the same velocity all over as the shape of the front changes over time.
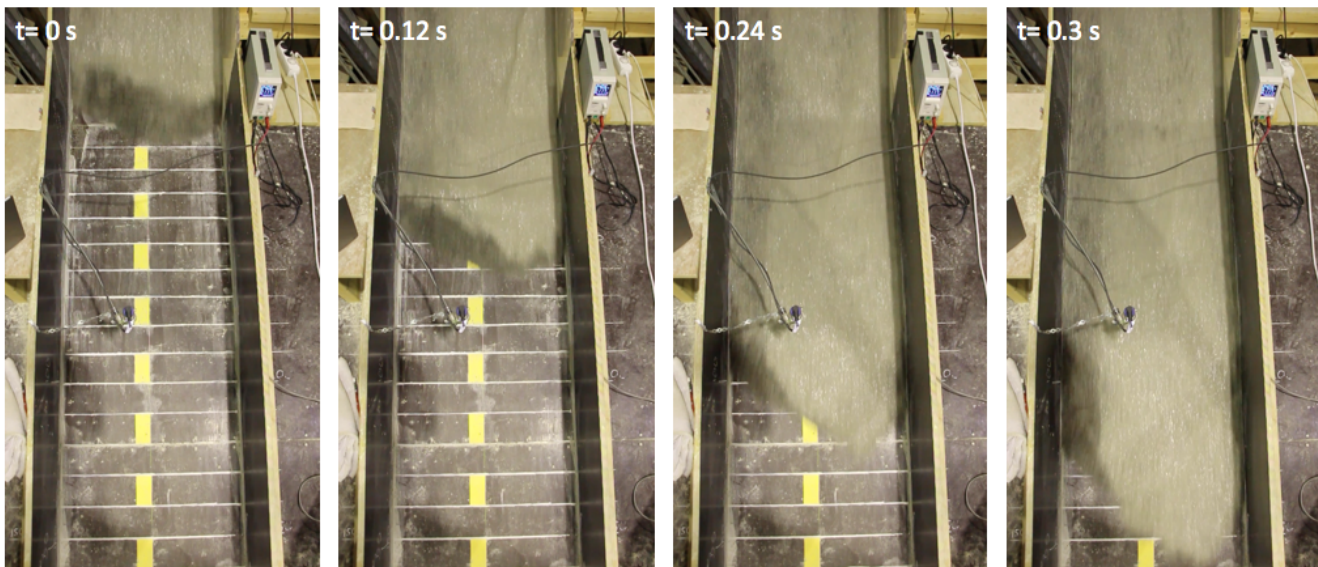
Figure 6.2: Four frames from the upstream camera from test 2 that illustrates the problem of the changing shape of debris flow front.

To keep the interpretation of the debris flow front velocity constant, the velocity was measured along the center line. However, this was not always where the front of the

debris flow front was situated. A better method would have been preferred as this method was time consuming and inaccurate. Despite this the velocity observed was close to what was expected considering the model laws and normal velocity values for debris flows.

6.1.2 Flow Height

The flow height was measured using an ultrasound sensor placed at x= -0.15 m. This sensor logged the height 13 times per second. Since it was fixed at one place the logged height gave a longitudinal profile of the passing debris flow. Figure 6.3 shows the flow height of tests 1-3.
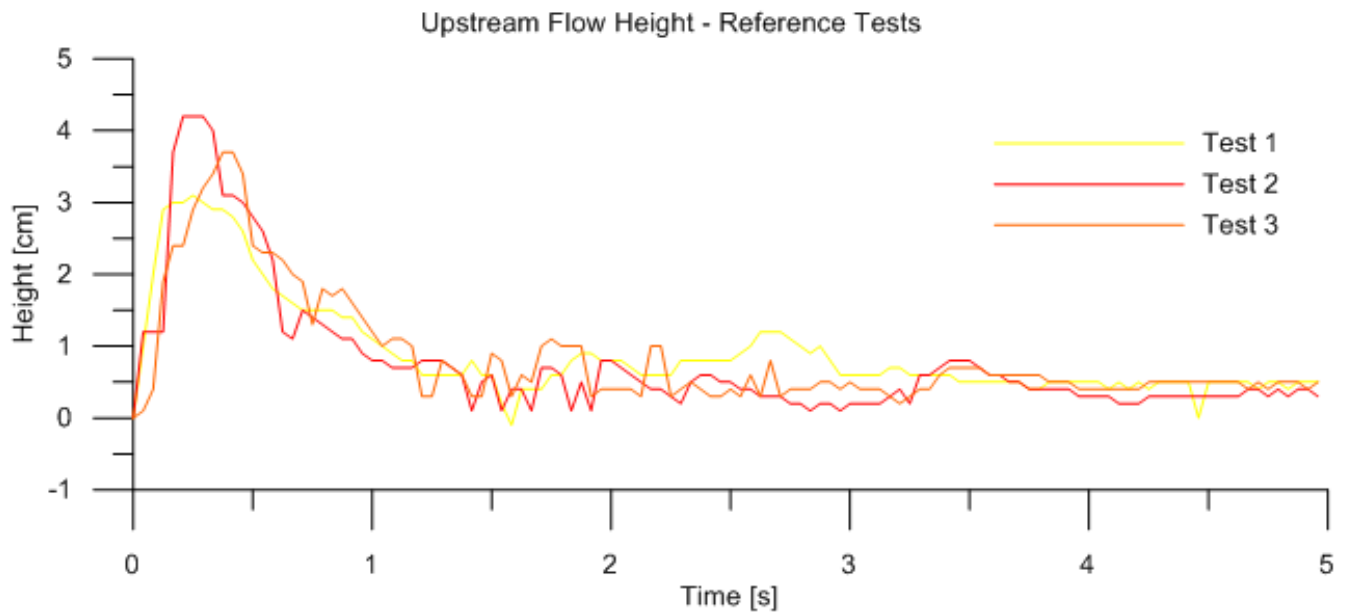
Figure 6.3: The logged debris flow height for the three reference tests.

The expected flow height calculated in section 4.1.1 for the physical modeled debris flow was 5 cm. For tests 1-3 the maximum observed flow height was between 3-4.25 cm. This flow height equals 0.6-0.85 m flow height for a real debris flow, which is close

to normal flow heights of debris flows. From the graphs in figure 6.3 it is visible that there is a debris flow front surge that is larger than the following surges of the debris flow body. These graphs corresponds to the theory presented in chapter 2 on how the debris flow act in surges. Either one large surge or several smaller surge. In this case there is one larger surge with smaller surges in the back. This could also explain why the velocity did not smoothly increase and decrease but instead had some variations as the main body would push the debris flow front in surges. It is believed that the debris flow front does not have excess pore fluid pressures as the main body does. There has not been any pore pressure measurements in these tests, so there is no way of saying if this is true for these tests. However, from the videos it looks as if the debris flow front in the beginning is dry and consists of "frozen masses" as Christiansen (2013) called it. This was a problem that she encountered which she thought was a result of the debris flow masses not being in suspension when released. Figure 6.4 is video frames from the upstream camera from tests 1-3 where the frozen masses are visible in the debris flow front as these are darker than the masses behind.
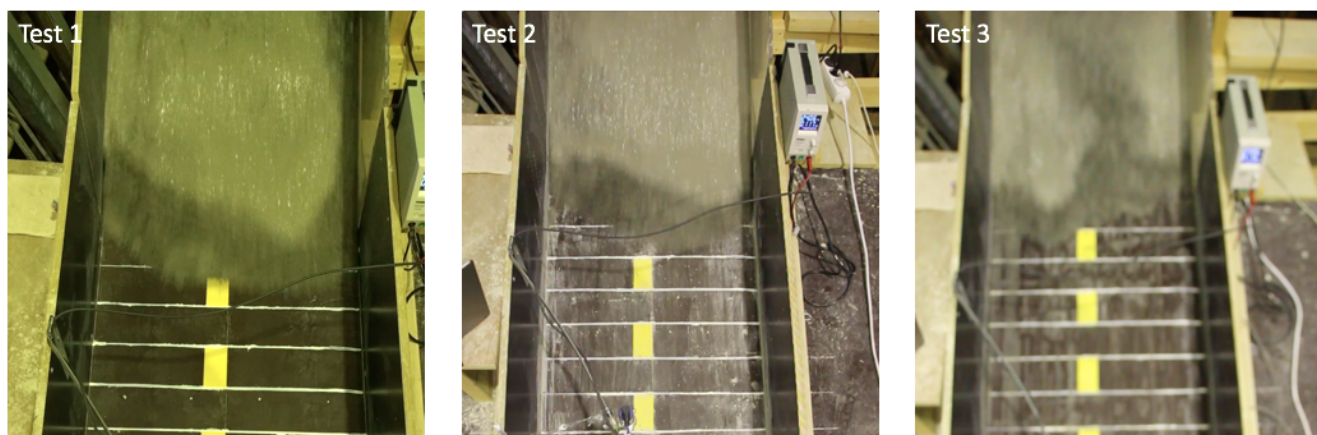
Figure 6.4: Frames from the upstream camera from test 1-3. The frozen masses in the debris flow front is visible as they are darker than the following the debris flow masses. This problem was also encountered by Christiansen (2013)

These frozen masses has a lower water content than the following masses and has a

higher internal friction and friction along the shear zone which caused energy loss. However, this dry debris flow front seem to disappear as it flows down the channel. By looking at the debris flow where it had its peak velocity one can observe that there is less visible frozen masses at this point than in the start of the channel. Figure 6.5 shows the tests 1-3 further down the channel than 6.4. The red line indicates x= -0.45 m which is where the highest velocity was recorded.
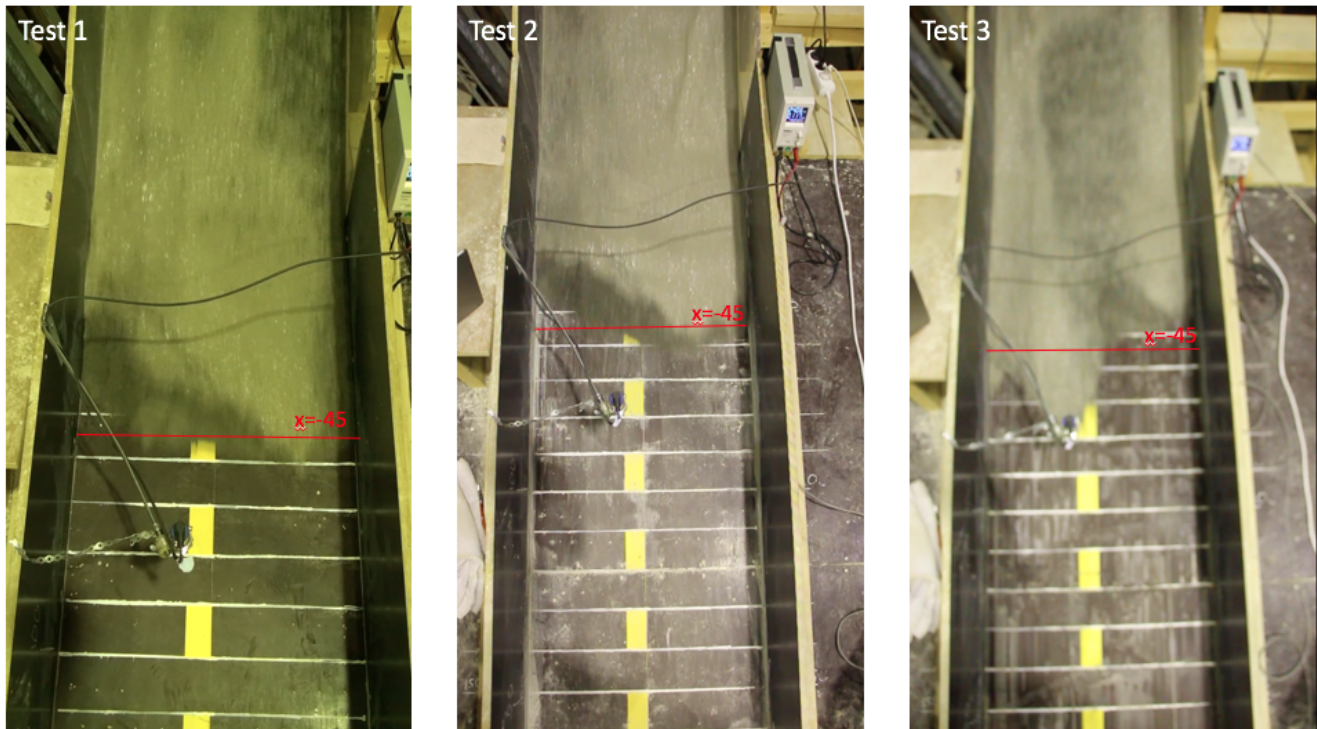
Figure 6.5: Frames from the upstream camera from test 1-3 where the red line indicates x=-0.45 m which is where the highest velocity was observed. The frozen masses are the darker areas of the debris flow, and is mainly observed in the debris flow front but is also occasionally visible in the following debris flow masses.

The debris flow accelerates up until x= -0.45 m this point and then decelerates until it stops on the runout table. The slope of the channel at this point is 13,8 degrees which is below the limit for of 16 degrees which is the slope that debris flow is most likely to occur. So, in relation to the velocity, if the debris flow masses had been properly in suspension from the release it might have reached its peak velocity at an earlier

time. In figure 6.5 it is also visible that there are some frozen masses in other part of the debris flow, not only in the front for test 1 and 2. There are some darker masses on the right of the debris flow in test 1 and some in the middle of test 3. This suggests that suspension problem is a problem for the whole mass and not only the debris flow front.

6.1.3 Energy Lines

The energy line of a debris flow normally has a slope between 0.2-0.3 for the lower part of the debris flow path according to Statens Vegvesen (2014). The energy lines of tests 1-3 are given in figure **??** and the average slope of the lower part of the path is given in table 6.1.

Table 6.1: Calculated average slope of the running average trend line of lower part of the energy lines for the reference tests 1-3.

Test	Average slope of the trend line
1	0.24
2	0.22
3	0.20

The value of the average slope falls within the normal values given by Statens Vegvesen (2014). This indicates that the model and the debris flow used could be a debris flow event in nature.
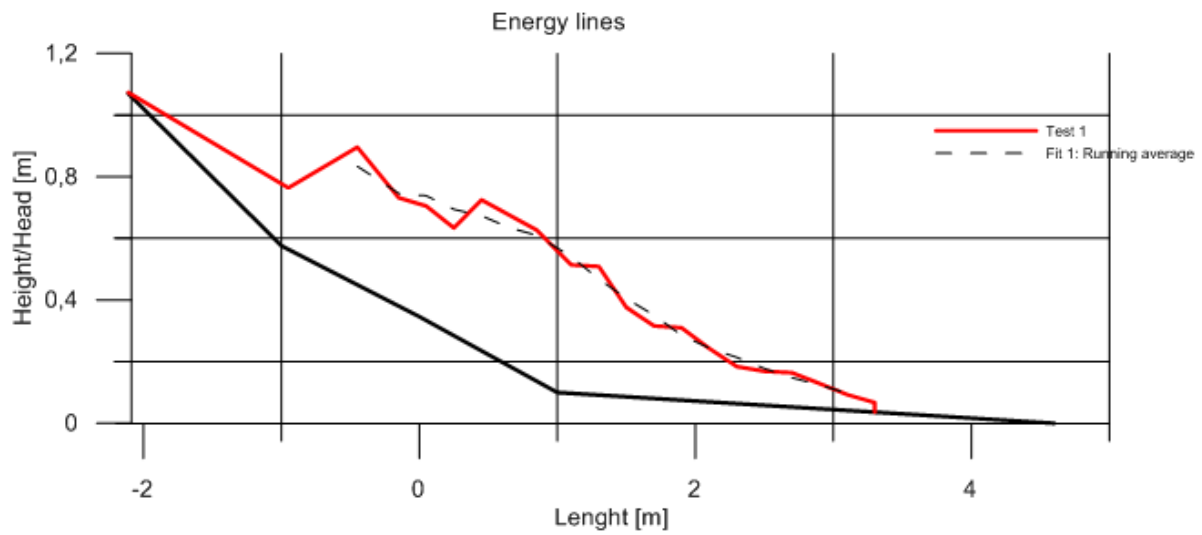
Figure 6.6: Energy lines for tests 1 and the trend line of the running average.
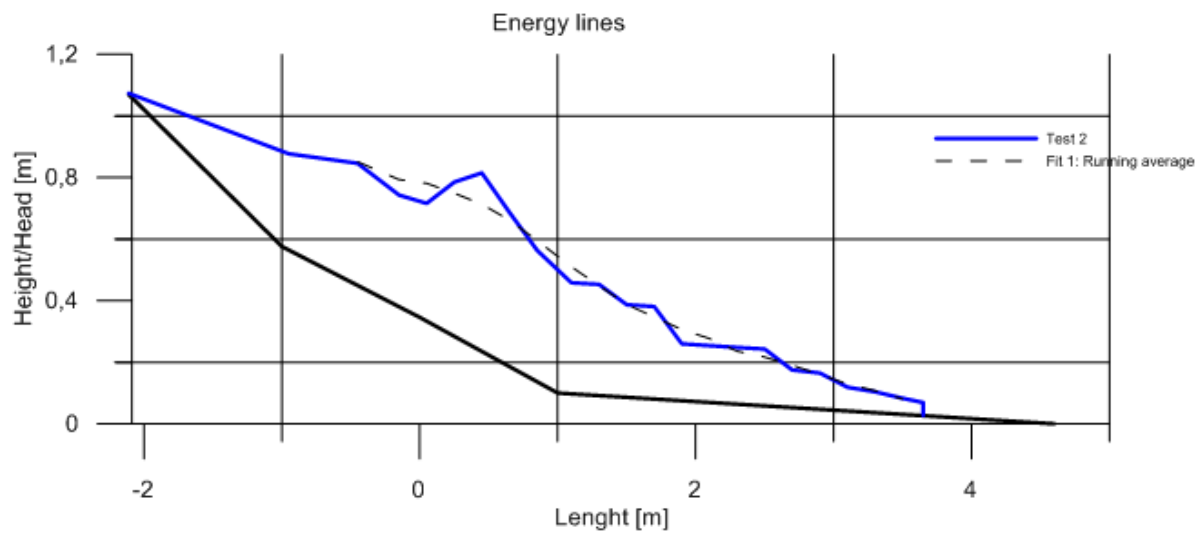
Figure 6.7: Energy lines for tests 2 and the trend line of the running average.
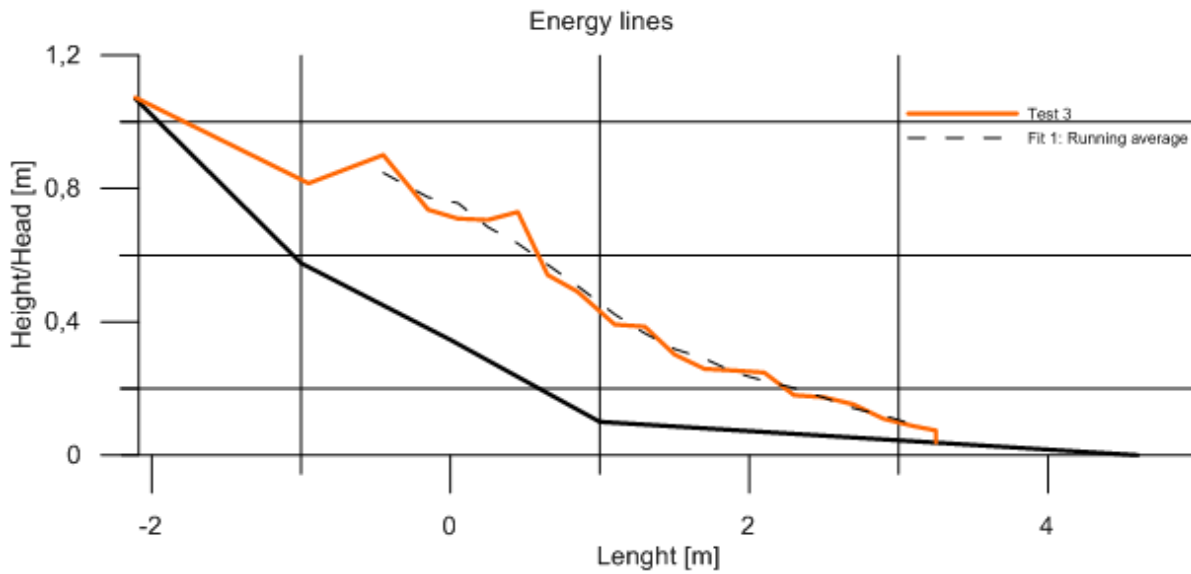
Figure 6.8: Energy lines for tests 3 and the trend line of the running average.

6.2 Debris Flow Breaker

The flow height of the debris flow front for the tests with the breakers was equal to the reference tests as seen in figure 5.13 and 5.14 presented in the results. A more interesting aspect of the flow height when the debris flow breakers was placed in the channel was the deposition height of the debris flow upstream of the debris flow breaker. Figure 6.9 shows the deposition height of all the tests with the different opening widths of the breaker.
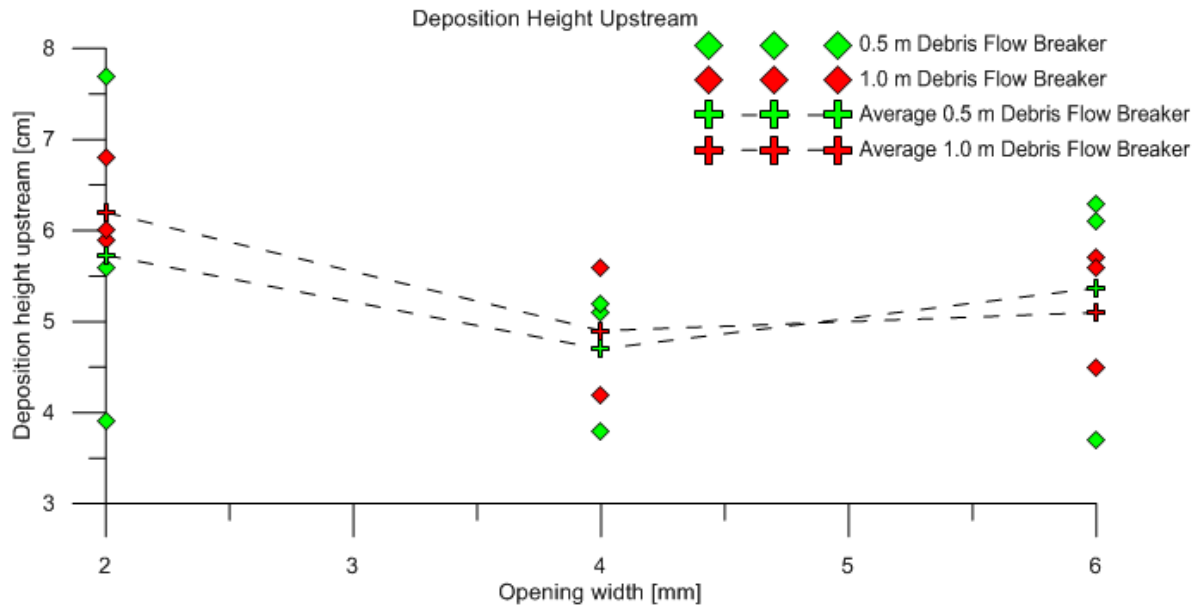
Figure 6.9: The deposition height of the debris flow upstream of the debris flow breaker with different opening widths.

There are large variations in the deposition height even for the same tests. However, for the average deposition height for the different opening widths it is clear that the 2 mm opening width breakers accumulate the most debris flow upstream. This accumulation is an interesting aspect of the debris flow breakers. From the videos one can observe debris flow accumulate and create a dam on top of the debris flow breaker as the debris flow flows. This dam grows larger as it accumulates more masses from the debris flow. Also, as the dam is located on the debris flow breaker the water drains through making the dam solid. Figure 6.10 are frames from the upstream camera for test 15. The red arrow indicated where the debris flow tail hits the accumulated dam and loses energy.
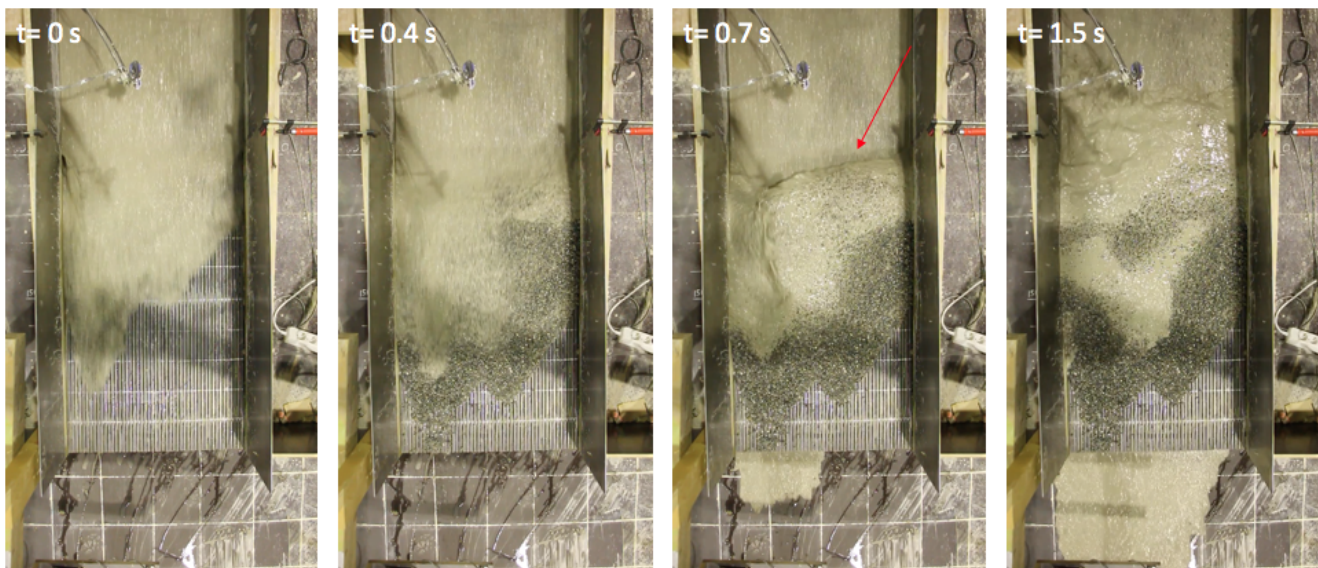
Figure 6.10: Frames from the video upstream of test 15 with the 1.0 m long breaker with 2 mm opening widths. The red arrow indicates where the debris flow hits the accumulated dam and causes the debris flow tail to stop.

The draining effect of the debris flow breaker can also be seen in figure 6.10. In frame t=0 s the debris flow front is fully saturated while in the three following frames the front has stopped on the breaker and for each frame it holds less water. Following the drainage of water is the after flow. This flow is also visible in the two last frames of figure 6.10. This after flow has not been given any focus in this work as it is assumed that it will not cause any harm to what it may encounter downstream. As mentioned earlier one example is that a road for example handle a water flow much better than a debris flow. Let alone, debris flows occur in established drainage paths where water already flows, so the additional water from the drained debris flow would not increase the existing flow remarkably.

On the other hand, for the 0.5 m long breakers the debris flow front did not stop on top of the breaker. The debris flow front flowed over the breaker and took a jump. However, the damming effect observed on the 1.0 m long breakers was also present

in the tests with the 0.5 m long breakers. Figure 6.11 shows both the jump and the damming effect. The red arrow indicates the accumulated dam.
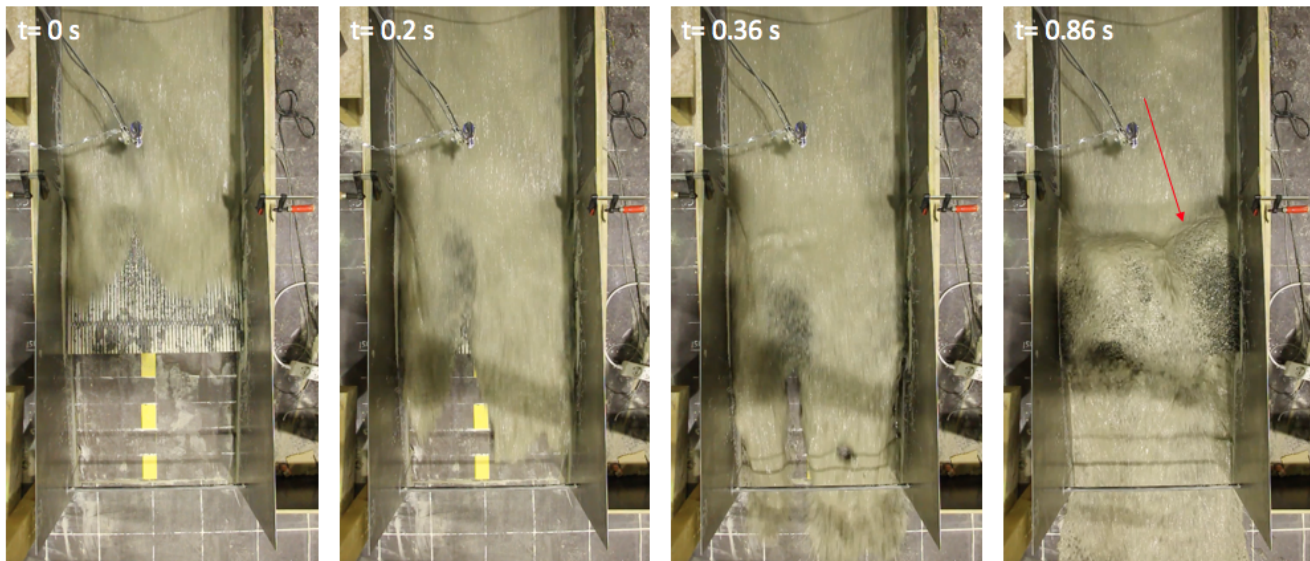
Figure 6.11

The average accumulated debris upstream of three different 0.5 m long breaker was only a few millimeters from the accumulated debris for the 1.0 m long breakers. But the variation in the deposition height for the 0.5 m breaker tests was larger than for the 1.0 m breaker tests. Table 6.2 shows the standard variation for the deposition height for the different breakers

Table 6.2: The average deposition height upstream of the different debris flow breakers.

Breaker	0.5 m		1.0 m	
	Average deposition height [cm]	Standard deviation [cm]	Average deposition height [cm]	Standard deviation [cm]
2 mm	5.73	1.90	6.2	0.49
4 mm	4.7	0.78	4.9	0.99
6 mm	5.37	1.45	5.1	0.60

This could also be interpreted as the 1.0 m long breaker being a more predictable countermeasure than the 0.5 m long breaker. When considering the effectiveness

in terms of the reduced runout compared to the reference tests, the 1.0 m breakers were all performing better than the 0.5 m long breaker. Figure 6.12 illustrates the effectiveness of the breakers in terms of reduced runout compared to the reference tests. The solid plates (0 mm opening width) are also included in this figure.
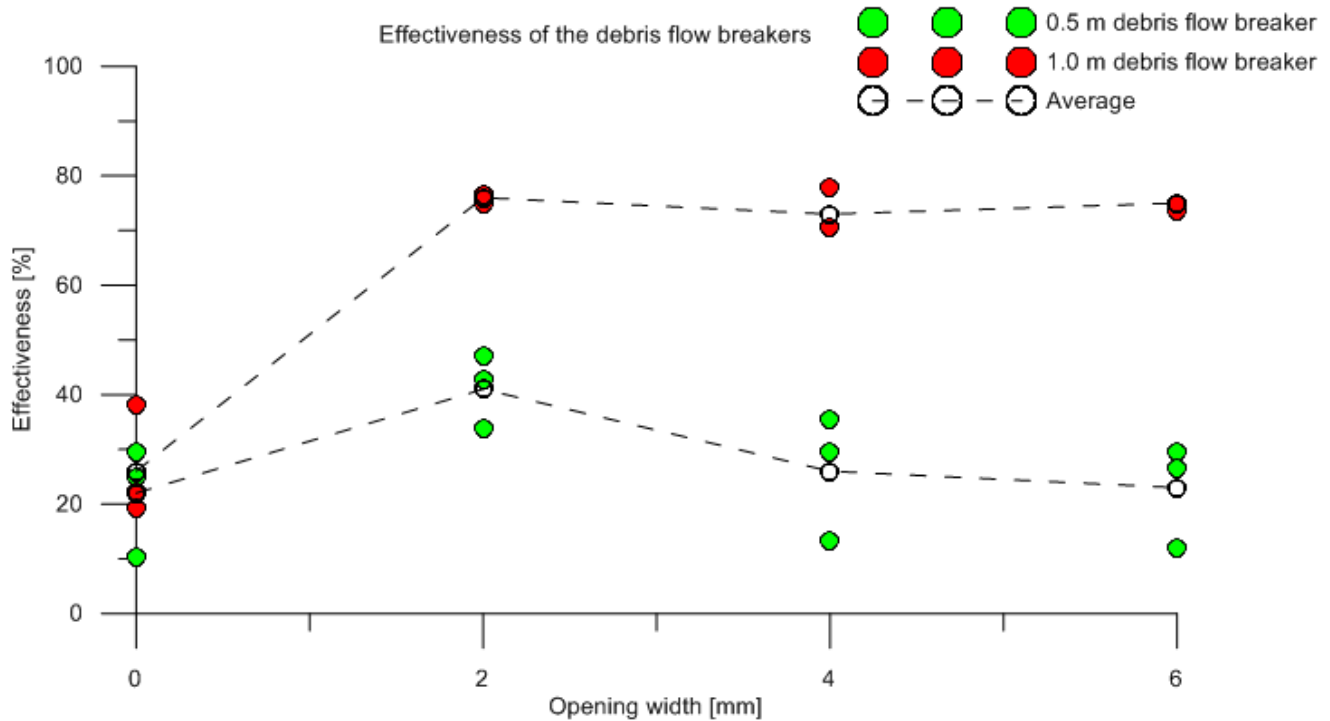
Figure 6.12: The effectiveness of the different breakers in terms of reduced runout compared to the reference tests.

From figure 6.12 one can see that all the tests with the 1.0 m breakers are more efficient than the 0.5 breaker tests. A larger variation in the runout for the 0.5 m breakers than for the 1.0 m breakers is also observed. The average runout and standard deviation for the breakers with an opening width is given in table 6.3.

Table 6.3: The average runout distance and standard deviation for the different breakers.

Breaker	0.5 m		1.0 m	
	Average runout [cm]	Standard deviation [cm]	Average runout [cm]	Standard deviation [cm]
0 mm	267	34	250	35
2 mm	200	23	82	3
4 mm	252	39	92	14
6 mm	263	32	87	3

The standard deviation for the 1.0 m solid plate (0 mm opening width) is in the same range as the standard deviation for all the 0.5 m long breakers. This indicates that the 1.0 m long breaker with an opening width larger than 0 mm is more predictable as it does not have larger variations for the same condition tests.

From the tests it is evident that length of the breaker should be 1.0 m to obtain the best effectiveness in terms of reduced runout. However, the opening width of the breaker does not seem to influence the effectiveness in such a large manner as the length. For the 1.0 m long breaker all opening width larger than 0 mm has an effectiveness around 75%. The opening width also determines the percentage opening due to the constant blocking width of the breakers and it is therefore not possible to determine if the percentage opening is an important factor influencing the effectiveness.

The results obtained through the physical experiments support the theory behind the debris flow breakers. This theory says that by removing the water one also removes the excess pore fluid pressures in the debris flow that created the low effective stresses along the shear zone. The results show that by going from a solid plate to a breaker with a 2 mm opening width the effectiveness increased by 25% for the 0.5 m breaker and 68% for the 1.0 m breaker. This indicates that by removing the water

thought the openings in the breaker, the debris flow stops due to the increase in effective stress along the shear zone. The test results indicate that 0.5 m long breaker does not provide sufficient length for the debris flow front to dissipate water through the openings as the front flows over the breaker and continues downstream. An interesting observation was that the 2 mm opening width was the only opening width of the 0.5 m long breaker that had a larger effectiveness than the solid plate. The 4 and 6 mm opening width had almost the same effectiveness as the solid plate. However, when looking at the deposition height it is observed that all the 0.5 m long breakers accumulate much debris flow upstream of the breaker. This indicate that the 0.5 m long breaker does not provide a sufficient length for the debris flow front to dissipate enough water to stop, but it is suffcient for the main debris flow body as this stops on the breaker where it creates the damming effect discussed earlier. One explanation for the longer runout observed for the 0.5 m long breaker with the 4 and 6 mm opening width could be the stronger after flow created by the drained water and material. Because, for the 4 and 6 mm opening widths around 90% of the debris flow can pass through the opening width, while for the 2 mm only 54% of the material can pass. This flow will therefore be weaker than the after flow created for the 4 and 6 mm opening width. The stronger after flow could therefore push the debris flow front further than the weaker after flow could and then create a longer runout. Material samples were taken to analyse what material would pass the debris flow and what material was held back. Table 6.4 gives the d_{50} of the downstream material which is the material of the debris flow front and the material that created the after flow.

Table 6.4: The d_{50} value of the material samples collected downstream

Debris Flow Breaker	d_50 downstream
(0.5 m - 2 mm)	1.0
(0.5 m - 4 mm)	1.4
(0.5 m - 6 mm)	1.6

These d_{50} values indicate that the after flow created when using the 4 and 6 mm opening width might be stronger than the after flow created by the 2 mm opening width due to the higher d_{50} value. In theory the same amount of water should be present in all the after flows as this passes throgh the opeing withs independent of the width. However, larger material has larger forces which can be the cause of the longer runout as the after flow pushes the debris flow front further.

When comparing the effectiveness of the debris flow breakers to other countermeasures tested in the same physical model it is clear that the many breakers are more effective than other countermeasures. Table 6.5 gives the effectivness in terms of reduced runout for the countermeasures tested by Fiskum (2012). The countermeasures tested by Christiansen (2013) were not possible to compare as she tested deflection structures and channels where the runout distance was not measured in the same manner.

Table 6.5: The effectivenesss of each countermeasure tested in the physical debris flow model. The effectiveness is measures in terms of reduced runout compared to the reference tests for the debris flow material used.

Countermeasure	Effectiveness
Debris flow breaker (0.5 m - 2 mm)	41%
Debris flow breaker (0.5 m - 4 mm)	26%
Debris flow breaker (0.5 m - 6 mm)	23%
Debris flow breaker (1.0 m - 2 mm)	76%
Debris flow breaker (1.0 m - 4 mm)	73%
Debris flow breaker (1.0 m - 6 mm)	75%
Check dam	67%
Slit dam (2 slits)	31%
Slit dam (4 slits)	42%
Baffle wall	14%
Slit dam and baffles (2 + 4)	44%
Slit dam and baffles (4 + 4)	40%
Baffles and wings	33%

Figure 6.13 shows the effectiveness of each countermeasure in a bar diagram. This diagram makes it easier to see which countermeasures are the most effective.
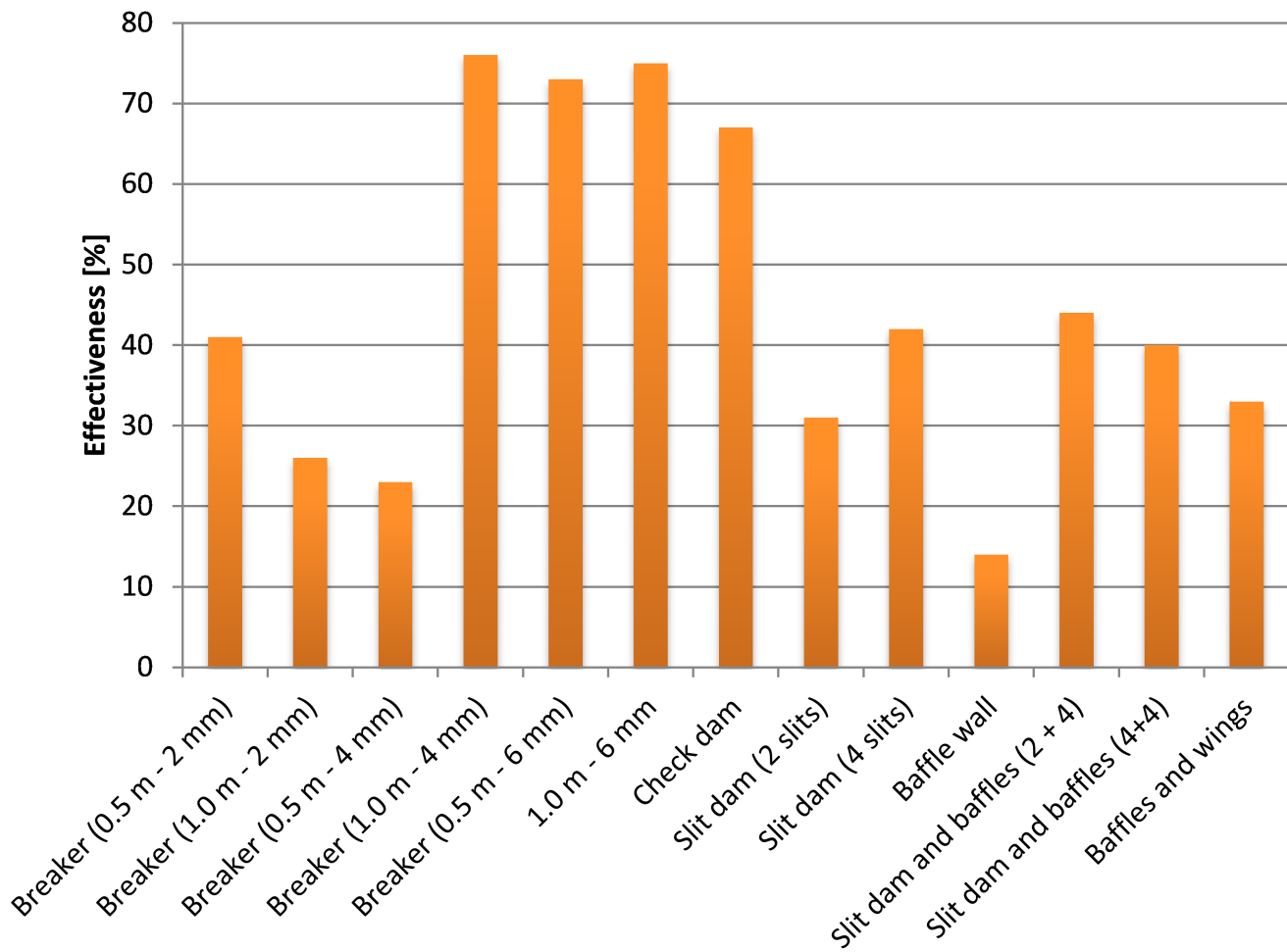
Figure 6.13: Bar diagram of the effectiveness of the different countermeasures in terms of reduced runout compared to their reference tests.

Both Fiskum (2012) and Christiansen (2013) used energy lines to evaluate the effectiveness of the countermeasures tested. The wanted outcome from the energy line analysis is a steeper slope on the countermeasure and downstream than upstream of the countermeasure. A steeper energy line means a higher energy loss over this distance. The energy lines obtained for the debris flow breakers were difficult to read and obtain the slope. A trend line of the running average was therefore added. The

slope of this line showed various results and did not give any useful information. This was probably due to the problematic reading of the velocity in the downstream area. A better velocity reading around the debris flow breaker would most probably give a more advantageous energy line because for the reference tests where there were not breaker the energy lines were readable and the slope was within the normal values of a real debris flow.

Chapter 7

Conclusion

In this chapter conclusions answering the objectives stated in chapter 1 will be given, and recommendations to further work.

7.1   Conclusions

Through the physical modeling, theory on the physics and process of debris flows had to be understood in order to evaluate whether the debris flow was realistic and could simulate an actual debris flow. The results from the reference tests showed results which were within the expected values for the debris flow front velocity, flow height and slope of the energy line.

The interaction between the debris flow breaker and the debris flow appeared to be as the theory suggested. The water drained through the opening widths and the debris flow front or body stopped on top of the breaker depending on the length of the

breaker. As the debris flow stopped the following part of the debris flow flowed into the stopped masses which were now dry. This damming effect caused the debris flow masses to accumulate upstream while the water drained through the dry masses and breakers. This upstream deposition height increased as the opening width of the debris flow breakers decreased. This was due to the opening width and material, for the 6 mm opening width 94% of the debris flow material could pass through the breaker while for the 2 mm opening width only 54% of the material could pass through.

The results from the 6 different debris flow breakers, excluding the solid plates which are not debris flow breakers, showed promising results. The 1.0 m long breakers were all more effective than the 0.5 m long breakers, regardless of the opening width. The effectiveness is measured in terms of reduced runout compared to the reference tests. The most effective debris flow breaker was the 1.0 m long breaker with 2 mm opening widths with an effectiveness of 76%. Since the blocking width was kept constant the percentage opening was not changed and the effect of this parameter was therefore not checked.

All three of the 1.0 m long breakers had a greater effectiveness than all other countermeasures tested in the physical model. These countermeasures included check dams, slit dams and baffles. The check dam had a effectiveness of 67% which was the closet to the 73-76% effectiveness the 1.0 m long breakers had. In conclusion, the results from the physical modeling of the debris flow breakers indicated that they are an effective countermeasure that should be trusted and used as a mitigation measure.

7.2   Recommendations for Further Work

Due to the difficult release of the debris flow in the existing model a new initiation method could be advantageous. One idea is to use a cement mixer and initialize the debris flow by pouring it out of the mixer. This would also solve the observed problem of frozen masses that is a result of separation in the suspension. If this could also remove the requirement of using a crane the process would be more flexible as there would not be necessary to have a licenced crane operator available for each test.

To study the pore pressure present in the debris flow along the flow path would be an important aspect to investigate in relation to debris flow breakers. By installing instruments to measure the pore pressure in the channel and on the debris flow breaker one could obtain valuable information about the excess pore pressure present in the debris flow and study more in detail the interaction between the debris flow and debris flow breaker.

For these experiments only one material was tested. To investigate the effectiveness of the breakers in-depth different material should be tested to see what effect the breakers have when the material changes.

How to implement the debris flow breaker in real life is also an important aspect to consider, a large scale physical experiment would be a good start.

A numerical model would also be interesting to develop and compare to the already existing models developed by Kim et al. (2012) and Gonda (2009).

.

Bibliography

Armanini, A., Dellagiacoma, F., and Ferrari, L. (1991). From the check dam to the development of functional check dams. In *Fluvial hydraulics of mountain regions*, pages 331–344. Springer.

Bagnold, R. A. (1954). Experiments on a gravity-free dispersion of large solid spheres in a newtonian fluid under shear. In *Proceedings of the Royal Society of London A: Mathematical, Physical and Engineering Sciences*, volume 225, pages 49–63. The Royal Society.

Brunella, S., Hager, W. H., and Minor, H.-E. (2003). Hydraulics of bottom rack intake. *Journal of Hydraulic Engineering*, 129(1):2–10.

Calligaris, C. and Zini, L. (2012). *Debris Flow Phenomena: A Short Overview?* INTECH Open Access Publisher.

Choi, C., Ng, C. W. W., Song, D., Kwan, J., Shiu, H., Ho, K., and Koo, R. (2014). Flume investigation of landslide debris–resisting baffles. *Canadian Geotechnical Journal*, 51(5):540–553.

Christiansen, L. F. (2013). Flomskred: Litteraturstudie og modellforsøk med voller som sikringstiltak.

Fiskum, E. (2012). Flomskred: Testing av ulike sikringstiltak i modellforsøk.

Gonda, Y. (2009). Function of a debris-flow brake. *International Journal of Erosion Control Engineering*, 2(1):15–21.

Hiller, P. and Jensen, L. (2009). Modellforsøk med flomskred mot bruer - virkning av bru
pning og ledevoller.

Hungr, O. (2005). Classification and terminology. In *Debris-flow hazards and related phenomena*, pages 9–23. Springer.

Hungr, O., Evans, S., Bovis, M., and Hutchinson, J. (2001). A review of the classification of landslides of the flow type. *Environmental & Engineering Geoscience*, 7(3):221–238.

Hungr, O., McDougall, S., and Bovis, M. (2005). Entrainment of material by debris flows. In *Debris-flow hazards and related phenomena*, pages 135–158. Springer.

ICHARM (2008). Debris-flow dewatering breakes: a promising tool for disaster management in developing countries. *International Centre for Water Hazard and Risk Management Newsletter*, 3.

Iverson, R. M. (1997). The physics of debris flows. *Reviews of geophysics*, 35(3):245–296.

Iverson, R. M., Reid, M. E., Logan, M., LaHusen, R. G., Godt, J. W., and Griswold, J. P. (2011). Positive feedback and momentum growth during debris-flow entrainment of wet bed sediment. *Nature Geoscience*, 4(2):116–121.

Kim, Y. (2013). Study on hydraulic characteristics of debris flow breakers and sabo dams with a flap.

Kim, Y., Nakagawa, H., Kawaike, K., and Zhang, H. (2012). Numerical and experimental study on debris flow breaker. *Disaster Prev Res Inst Annals*, 55(B):471–481.

Kuntzmann, J. and Bouvard, M. (1954). Étude théorique des grilles de prises d'eau du type «en-dessous». *La Houille Blanche*, (5):569–574.

Laache, E. (2015). Effective debis flow countermeasures: A literature review of debris flow countermeasures.

LCWConsult (2015). Slit dams in sta luzia stream for debris flow.

Lygre, E. T. (2014). Skred på norske veier. *Teknisk Ukeblad*.

Major, J. J. and Iverson, R. M. (1999). Debris-flow deposition: effects of pore-fluid pressure and friction concentrated at flow margins. *Geological Society of America Bulletin*, 111(10):1424–1434.

McArdell, B. W., Bartelt, P., and Kowalski, J. (2007). Field observations of basal forces and fluid pore pressure in a debris flow. *Geophysical Research Letters*, 34(7).

Mizuyama, T. (2008). Structural countermeasures for debris flow disasters. *International Journal of Erosion Control Engineering*, 1(2):38–43.

Orth, J., Chardonnet, E., and Meynardi, G. (1954). Étude de grilles pour prises d'eau du type «en dessous». *La Houille Blanche*, (3):343–351.

Ract-Madoux, X., Bouvard, M., Molbert, J., and Zumstein, J. (1955). Quelques réalisations récentes de prises en-dessous à haute altitude en savoie. *La Houille Blanche*, (6):852–878.

Remaître, A., Van Asch, T. W., Malet, J.-P., and Maquaire, O. (2008). Influence of check dams on debris-flow run-out intensity. *Natural Hazards and Earth System Science*, 8(6):1403–1416.

Sandersen, F., Bakkehøi, S., Hestnes, E., and Lied, K. (1997). The influence of meteorological factors on the initiation of debris flows, rockfalls, rockslides and rockmass stability. *Publikasjon-Norges Geotekniske Institutt*, 201:97–114.

Sassa, K., Fukuoka, H., Wang, G., and Wang, F. (2007). Undrained stress-controlled dynamic-loading ring-shear test to simulate initiation and post-failure motion of landslides. In *Progress in landslide science*, pages 81–98. Springer.

Statens Vegvesen (2014). Håndbok v139: Flom- og sørpeskred. *Vegdirektoratet, Oslo.*

Stiny, J. (1910). *Die Muren: Versuch einer Monographie mit besonderer Berücksichtigung der Verhältnisse in den Tiroler Alpen.* Wagner.

Takahashi, T. (2014). *Debris flow: mechanics, prediction and countermeasures.* CRC Press.

Thomas, D. S. and Goudie, A. S. (2009). *The dictionary of physical geography.* John Wiley & Sons.

VanDine, D. (1996). Debris flow control structures for forest engineering. *Res. Br., BC Min. For., Victoria, BC, Work. Pap*, 8:1996.

Volkwein, A. (2014). Flexible debris flow barriers - design and application. page 29.

Volkwein, A., Wendeler, C., and Guasti, G. (2011). Design of flexible debris flow barriers. *Italian J Eng Geol Environ. doi*, 10(4408):2011–03.

Wang, G. and Sassa, K. (2003). Pore-pressure generation and movement of rainfall-induced landslides: effects of grain size and fine-particle content. *Engineering geology*, 69(1):109–125.